The Exocyst Functions in Niche Cells to Promote Germline Stem Cell Differentiation by Directly Controlling EGFR Membrane Trafficking

Ying Mao[1#], Renjun Tu[2#], Yan Huang[3#], Decai Mao[1], Zhihao Yang[1], Pik Ki Lau[3], Jinhui[3] Wang, Jianquan Ni[1*], Yusong Guo[3*] and Ting Xie[2*]

[1]PKU-THU Joint Center for Life Sciences, College of Life Sciences, School of Medical Sciences, Tsinghua University, Beijing 100084, China.

[2]Stowers Institute for Medical Research, 1000 East 50th Street, Kansas City, MO 64110, USA

[3]Division of Life Science, Hong Kong University of Science and Technology, Clear Water Bay, Kowloon, Hong Kong, China

[#]Those authors contributed equally

*Correspondence: Ting Xie, tgx@stowers.org; Yusong Guo, guoyusong@ust.hk; Jianquan Ni, nijq@mail.tsinghua.edu.cn

Abstract

The niche controls stem cell self-renewal and differentiation in animal tissues. Although the exocyst is known to be important for protein membrane trafficking and secretion, its role in stem cells and niches has never been reported. Here, this study shows that the exocyst functions in the niche to promote germline stem cell (GSC) progeny differentiation in the *Drosophila* ovary by directly regulating EGFR membrane trafficking and signaling. Inactivating exocyst components in inner germarial sheath cells, which form the differentiation niche, causes a severe GSC differentiation defect. The exocyst is required for maintaining niche cells and preventing BMP signaling in GSC progeny by promoting EGFR membrane targeting and signaling through direct association with EGFR. Finally, it is also required for EGFR membrane targeting, recycling and signaling in human cells. Therefore, this study has revealed a novel function of the exocyst in niche cells to promote stem cell progeny differentiation by directly controlling EGFR membrane trafficking and signaling *in vivo*, and has also provided important insight into how the niche controls stem cell progeny differentiation at the molecular level.

Introduction

In adult tissues, stem cells continuously self-renew and differentiate to produce functional differentiated cells for replenishing lost cells caused by injury, disease or aging. Studies in *Drosophila* and mammals have shown that stem cell self-renewal is tightly controlled by the concerted actions of the niche and intrinsic factors (Fuller and Spradling, 2007; Li and Xie, 2005; Morrison and Spradling, 2008; Xie, 2013). Based on our recent finding in the *Drosophila* ovary, we propose that stem cell progeny differentiation is also controlled by a distinct "differentiation niche" (Kirilly et al., 2011). Recent studies from our lab and others have further confirmed the existence of the differentiation niche (Fu et al., 2015; Li et al., 2015; Liu et al., 2010; Liu et al., 2015; Lu et al., 2015; Luo et al., 2015; Ma et al., 2014; Wang et al., 2015; Wang et al., 2011). However, it remains largely unknown how this new niche controls GSC progeny differentiation at the molecular level.

The *Drosophila* ovary is an attractive system for studying stem cell regulation in relationship to niches because of well-defined GSC lineage and surrounding somatic cells (Spradling et al., 2011; Xie, 2013). At the apical tip of the ovary lie 12-16 germaria , each carrying 2-3 GSCs (Lin and Spradling, 1993; Spradling, 1993). In the germarium, 5-7 cap cells and GSC-contacting anterior inner germarial sheath cells (ISCs, previously known as escort cells) form the niche for promoting GSC self-renewal (Kirilly et al., 2011; Wang et al., 2011; Xie and Spradling, 2001; Xie and Spradling, 2000). Niche-derived BMP-like Dpp directly controls GSC self-renewal by repressing differentiation (Chen and McKearin, 2003; Song et al., 2004; Xie and Spradling, 1998), while E-cadherin-

mediated cell adhesion helps anchor GSCs in the niche for long-term self-renewal (Song et al., 2002). Therefore, the niche controls GSC self-renewal by providing anchorage and repressing differentiation.

Each GSC division generates a differentiating cystoblast (CB), which then undergoes four synchronous divisions to produce an interconnected 16-cell cyst with mitotic 2-cell, 4-cell and 8-cell intermediates. The CBs, mitotic intermediates and 16-cell cysts are encased by ISC cellular processes in the anterior germarium (Decotto and Spradling, 2005; Kirilly et al., 2011; Morris and Spradling, 2011). *bam* is repressed by BMP signaling in GSCs, and is upregulated in CBs and mitotic cysts (Chen and McKearin, 2003; Song et al., 2004). Bam promotes GSC progeny differentiation by working with other differentiation factors (Xie, 2013). In addition to the Bam-dependent intrinsic mechanisms, the ISC-based differentiation niche promotes GSC progeny differentiation extrinsically (Kirilly et al., 2011). The studies from us and others have demonstrated that ISC cellular process-mediated direct interactions are critical for GSC progeny differentiation (Banisch et al., 2017; Kirilly et al., 2011; Lu et al., 2015; Maimon et al., 2014; Su et al., 2018; Wang et al., 2015; Wang et al., 2011). In addition, the elimination of ISCs results in the most severe germ cell differentiation defect, further supporting the critical importance of ISCs in promoting GSC progeny differentiation (Kirilly et al., 2011; Wang et al., 2015; Wang and Page-McCaw, 2018; Wang et al., 2011). Mechanistically, ISCs promote GSC progeny differentiation by preventing BMP signaling through multiple mechanisms. EGFR signaling operates in ISCs to prevent BMP signaling by repressing *dally*, encoding a proteoglycan for facilitating Dpp

diffusion (Liu et al., 2010), while Wnt signaling functions in ISCs to prevent BMP signaling by maintaining BMP receptor Tkv-mediated Dpp trapping and ISC survival (Luo et al., 2015; Mottier-Pavie et al., 2016; Wang et al., 2015). In addition, Rho prevents BMP signaling by repressing *dally* and *dpp* in ISCs, whereas Eggless, Piwi, Lsd1, Hh signaling and the COP9 complex repress *dpp* in ISCs (Eliazer et al., 2014; Eliazer et al., 2011; Huang et al., 2017; Jin et al., 2013; Kirilly et al., 2011; Liu et al., 2015; Lu et al., 2015; Ma et al., 2014; Wang et al., 2015; Wang et al., 2011). Tkv acts in ISCs to prevent Dpp diffusion and promote Hh signaling, thereby preventing BMP signaling (Luo et al., 2015; Tseng et al., 2018). Thus, ISCs promote GSC progeny differentiation primarily by preventing BMP signaling.

Long ISC cellular processes should behave like invadosomes because they have to retract from a departing cyst and extend to a new passing-by cyst (Kirilly et al., 2011; Morris and Spradling, 2011). Exocytosis can provide the membrane for protrusion (Bretscher, 2008). In *Drosophila*, exocytosis is controlled by the highly conserved exocyst complex genes, including *sec5*, *sec6*, *sec10* and *sec15* (Langevin et al., 2005; Murthy et al., 2003; Murthy et al., 2005). In this study, we show that the exocyst is required in ISCs themselves to maintain ISCs and their long cellular processes as well as promote GSC progeny differentiation by directly regulating EGFR membrane trafficking and signaling. Moreover, polarized exocytosis toward apical side of ISCs observed in this study might also provide important insights into the generation and maintenance of ISC cellular processes.

Results

Exocyst components are required in ISCs to promote GSC progeny differentiation

To determine the function of the exocyst in the differentiation niche of the *Drosophila* ovary, we used the ISC-expressing *c587-gal4* driver and *UAS-RNAi* transgenic strains to knock down *sec5*, *sec6*, *sec10*, and *sec15* specifically in ISCs. The ovaries from the control and *sec* knockdown females were labeled for Hu-li tai shao (Hts), and were quantified for GSC and CB numbers. Hts labels the spherical spectrosome in GSCs/CBs and the branched fusome in cysts (Lin et al., 1994); GSCs can be distinguished from CBs by their direct contact with cap cells (Xie and Spradling, 2000). The control germaria usually contain 2 or 3 GSCs and one CB (Fig. 1A, 1F). Although the *sec5*, *sec6*, *sec10* and *sec15* knockdown (*sec5-i*, *sec6-i*, *sec10-i* and *sec15-i*, respectively) germaria contain 2 or 3 GSCs as in the control germaria, they carry significantly more spectrosome-containing single germ cells (thereafter referred to as SGCs), which lie posterior to GSCs, than those of control germaria, indicating that exocyst components are required in ISCs to promote CB differentiation (Fig.1B-F). To further determine their requirements in adult ISCs for promoting CB differentiation, we used *c587-gal4*, *tubulin-gal80^{ts}* (adult females, which were obtained at 25^{o}C to allow Gal80^{ts} to repress Gal4-driven RNAi knockdown, were then shifted to 29^{o}C for inactivating Gal80^{ts} and permitting Gal4-driven RNAi knockdown) to knock down the exocyst complex specifically in adult ISCs because *c587* is also expressed in developing ISCs. The two-week *sec5*, *sec6*, *sec10* and *sec15* knockdown ovaries accumulate much more SGCs than those one-week knockdown ovaries, and they also carry as many SGCs

as those knockdown ovaries from females cultured at 29°C throughout development (Fig. 1G-L). These results demonstrate that exocyst components are also required in adult ISCs to promote GSC progeny differentiation.

Two independent approaches were used to confirm that the germ cell differentiation defects are indeed caused by *sec* gene knockdown. First, our quantitative RT-PCR results show that the mRNA expression of *sec5*, *sec6*, *sec10* and *sec15* in the isolated germaria is efficiently and significantly knocked down by corresponding RNAi lines (Fig. S1). Second, ISC-specific expression of RNAi-resistant *sec10-GFP* (carrying the nucleotide changes for preventing knockdown, but still encoding a wild-type Sec10 protein) can sufficiently and fully rescue the germ cell differentiation defect caused by *sec10* knockdown (Fig. 1M-O). This result also indicates that the C-terminal GFP tagged Sec10 is also functional. Since knocking down four exocyst components produces similar germ cell differentiation defects, these results demonstrate that exocyst components are required in ISCs to promote GSC progeny differentiation.

To rule out the possibility that *sec* knockdown ISCs are functionally converted into cap cells known to promote self-renewal and repress differentiation (Song et al., 2007; Ward et al., 2006; Xie and Spradling, 2000), we used Lamin C as a molecular marker to identify cap cells in the control and *sec* knockdown ovaries (Xie and Spradling, 2000) (Fig. S2A). Interestingly, the *sec5-i*, *sec6-i*, *sec10-i* and *sec15-i* ISCs did not express Lamin C, and knocking down these *sec* genes in ISCs does not change the endogenous cap cell number or produce ectopic cap cells (Fig. S2B-D). These results

indicate that the germ cell differentiation defects caused by *sec* knockdown in ISCs are unlikely due to the formation of more or ectopic cap cells.

The exocyst is required for the polarized transport of cellular vesicles in ISCs

The exocyst is known to be associated with secreted vesicles (SVs) to regulate their membrane tethering in *Drosophila* and other systems (Langevin et al., 2005; Wu and Guo, 2015). To determine if exocyst components are associated with cellular vesicles, we used Sec10-GFP and Sec15-GFP to visualize the subcellular localization of the exocyst in ISCs. Sec10-GFP shows strong punctate staining underneath the cytoplasmic membrane, which most likely represent individual cellular vesicles (Fig. 2A and 2A'). Interestingly, these punctate speckles in ISCs are mostly restricted to the apical areas facing germ cells and lying underneath long cellular protrusions. Sec15-GFP, the protein trap line in which GFP is fused in frame with Sec15 protein, should recapitulate endogenous Sec15 protein expression pattern (Kelso et al., 2004). Interestingly, Sec15-GFP is also primarily expressed in ISCs (Fig. 2B). Consistent with Sec10-GFP subcellular localization in ISCs, Sec15-GFP also exhibits punctate speckles under the surface areas facing germ cells and long cellular protrusions (Fig. 2B and 2B'). These observations suggest that the exocyst is associated with cellular vesicles in ISCs.

To determine if the exocyst is required for membrane vesicle trafficking in ISCs, we examined the expression of Sec10-GFP and Sec15-GFP in *sec* knockdown ISCs. Interestingly, *sec5* and *sec15* knockdown ISCs lose the Sec10-GFP punctate staining patterns under the cytoplasmic membrane, and instead exhibit uniform Sec10-GFP

protein distribution in the cytoplasm (Fig. 2C and 2D). Consistently, *sec5* and *sec6* knockdown ISCs show the uniform Sec15-GFP protein distribution in the cytoplasm (Fig. 2E and 2F). Sec10-GFP- and Sec15-GFP-associated cellular vesicles are also localized to their basal side of the *sec* knockdown ISCs, which is in contrast with the control ISCs showing very few Sec10/15-positive vesicles on the basal side (Fig. 2C-F). In addition, some knockdown ISCs also completely lose the Sec10-GFP or Sec15-GFP expression, which might be caused by protein degradation due to the loss of other exocyst components (Fig. 2C-F). Taken together, exocyst components are important for polarized vesicle trafficking and also possibly important for one another's stability in ISCs.

The exocyst maintains ISCs by promoting cell proliferation and survival

As shown previously (Lu et al., 2015; Wang et al., 2015), *c587-gal4*-driven *UAS-RNAi* knockdown exhibits the temperature-sensitive nature: little or no knockdown at 18ºC and efficient knockdown at 29ºC. Consistently, *sec5-i, sec6-i, sec10-i and sec15-i* germaria of the females raised at 18ºC carry the normal numbers of ISCs and CBs as in the control germaria, indicating that these ISCs develop normally and have normal function for supporting GSC progeny differentiation (Fig. S3A-F'). After the adult females were cultured at 29ºC for 2 and 4 weeks, the *sec5-i, sec6-i, sec10-i and sec15-i* germaria accumulate significantly more SGCs than the control germaria, further supporting that the exocyst is required in adult ISCs to promote GSC progeny differentiation (Fig. 3A-C, 3E-G). Intriguingly, the 25-to-29ºC shift-based $Gal80^{ts}$-based conditional *sec* gene knockdown produces stronger knockdown phenotypes than the 18-to-29ºC-based knockdown two weeks after 29ºC because the former strategy has the

leaked expression causing moderate germ cell differentiation defects even at 25°C (Fig. S3G-L). Thus, the 18-to-29°C conditional knockdown strategy is utilized for all the later experiments. Additionally, a PZ1444 LacZ reporter is also used for quantifying ISCs because it labels both ISCs and cap cells, which can be reliably distinguished according to their physical localization and cell size (Margolis and Spradling, 1995; Xie and Spradling, 2000). The *sec5-i, sec6-i, sec10-i and sec15-i* germaria have significantly fewer ISCs than the control germaria (Fig. 3D, 3H). These results indicate that the exocyst is required for maintaining adult ISCs and promoting GSC progeny differentiation.

ISCs undergo slow turnover, and lost ISCs can be replenished by the proliferation of their neighboring ISCs (Kirilly et al., 2011). To determine if ISC loss is caused by defective cell proliferation, apoptosis or both, we used BrdU and TUNEL labeling to examine the proliferation and apoptosis of control and *sec* knockdown ISCs, respectively. Following 3-day BrdU feeding, about 20% of the control ISCs are BrdU-positive (Figure 3I, 3K). By contrast, *sec5-i, sec6-i, sec10-i* and *sec15-i* ISCs show significantly lower BrdU-positive rates than the control ISCs, and thus the *sec* knockdown germaria contain fewer BrdU-positive ISCs (Figure 3J, 3K). About 0.7% of the control ISCs are positive for TUNEL labeling (Fig. 3L, 3N). By contrast, *sec5-i, sec6-i, sec10-i* and *sec15-i* germaria tend to have more TUNEL-positive ISCs than the control ones (Fig. 3M, 3N). The cell death inhibitor *p35* is known to prevent apoptosis in *Drosophila* when overexpressed (Hay et al., 1994). Consistently, *p35* overexpression can significantly prevent the loss of *sec5-i*, *sec6-i* and *sec10-i* ISCs, and can also significantly rescue the

germ cell differentiation defects caused by *sec* knockdown (Fig. 3O-R). These results indicate that exocyst components promote ISC maintenance via regulation of cell survival and proliferation.

The exocyst is required in ISCs to promote GSC progeny differentiation partly by preventing BMP signaling

ISCs have been shown to shield GSC progeny from BMP signaling by repressing *dpp* expression or preventing its diffusion (Kirilly et al., 2011; Liu et al., 2010; Lu et al., 2015; Ma et al., 2014; Wang et al., 2011). BMP signaling activities can be monitored by the expression of phosphorylated Mad (pMad), *Dad-lacZ* and *bam-GFP* (Chen and McKearin, 2003; Song et al., 2004; Xie and Spradling, 1998). In the control germaria, GSCs express pMad and *Dad-lacZ* but not *bam-GFP*, and CBs and mitotic cysts express *bam-GFP*, but low or no pMad and *Dad-lacZ* (Fig. 4A-A"). By contrast, in the *sec5-i*, *sec6-i* and *sec15-i* germaria, those accumulated SGCs lying posteriorly to GSCs often upregulate pMad and *Dad-lacZ* expression and frequently downregulate *bam-GFP* expression (Fig. 4B-D"). Based on the expression of pMad, *Dad-lacZ* and *bam-GFP*, some of the accumulated SGCs in the *sec* knockdown germaria resemble GSCs, and most of them are CB-like, suggesting that those accumulated SGCs are a mixture of GSC-like and CB-like cells. These results further support that the exocyst is required in ISCs to promote GSC progeny differentiation by preventing BMP signaling.

To investigate if the exocyst is required in ISCs to prevent BMP signaling by repressing *dpp* expression, we used RT-PCR to examine *dpp* mRNA expression in the purified control and knockdown ISCs. Interestingly, *dpp* is significantly upregulated in the *sec6-i, sec10-i and sec15-i* ISCs compared with the control (Fig. 4E). As we reported previously (Lu et al., 2015; Ma et al., 2014; Wang et al., 2011), *dpp* knockdown in adult ISCs have no visible effect on GSC maintenance and GSC progeny differentiation using two independent RNAi lines (Fig. 4F and 4F'). The *sec5-i dpp-i*, *sec6-i dpp-i*, *sec10-i dpp-i* and *sec15-i dpp-i* double knockdown germaria contain significantly less SGCs than the *sec5-i*, *sec6-i*, *sec10-i* and *sec15-i* germaria, respectively, indicating that ISC-specific *dpp* knockdown significantly rescues the germ cell differentiation defects caused by *sec* gene knockdown (Fig. 4G-I). Interestingly, *dpp* knockdown can also partially and significantly prevent the ISC loss caused by *sec6/10* knockdown, suggesting that upregulated BMP signaling also contributes to the ISC loss (Fig. 4J-L). These results indicate that the exocyst is required in ISCs to repress *dpp* expression and thereby promote GSC progeny differentiation.

The exocyst is required for maintaining long ISC cellular processes

Long ISC cellular protrusions are required to promote GSC progeny differentiation in the *Drosophila* ovary (Kirilly et al., 2011; Lu et al., 2015). To determine if the exocyst is required to maintain long ISC cellular processes, we used *c587-gal4*-driven expression of membrane-tethered CD8-GFP in control and *sec*

knockdown ISCs. In the control germaria, long GFP-positive ISC cellular processes wrap around the differentiated GSC progeny (Fig. 5A). By contrast, the *sec5-i*, *sec10-i* or *sec15-i* ISCs lack long cellular processes that encase differentiated GSC progeny (Fig. 5B-D). These results indicate that the exocyst is required for the maintenance of long ISC cellular processes.

Since the loss of long ISC cellular processes could be a consequence of the germ cell differentiation defects caused by *sec* knockdown (Kirilly et al., 2011), we used the flipase-mediated FLP-out system to label individual control and *sec* knockdown ISCs with GFP in adulthood to determine if exocytosis is required to maintain long ISC cellular processes. In the FLP-out system, one heatshock treatment results in the removal of the transcription stop sequence between the *actin5C* promoter and the yeast *gal4* gene, thereby turning on the expression of *gal4*, which then drives *UAS-GFP* expression for labeling individual somatic cells, including ISCs (Ito et al., 1997). In the control, GFP-marked individual control ISCs often have long cellular processes, however, but some of them have short or no cellular processes, indicating that ISCs likely retract and extend their cellular processes while encasing the bypassing differentiated GSC progeny (Fig. 5E and 5I). Short ISC cellular processes are defined as those wrapping less than half of the underlying cysts, as long cellular processes of individual ISCs can fully cover the underlying cysts (Kirilly et al., 2011). Interestingly, the GFP-labeled *sec5-i*, *sec6-i*, *sec10-i* and *sec15-i* ISCs more frequently have no or only short cellular processes compared to those control ones (Fig. 5F-I). These results demonstrate that the exocyst is required intrinsically to maintain long ISC cellular processes.

Exocyst components are also required to maintain EGFR-MAPK signaling in ISCs

EGFR-MAPK signaling operates in ISCs to promote GSC progeny differentiation (Liu et al., 2010; Schultz et al., 2002). MAPK signaling activity is normally monitored by the expression of phosphorylated MAPK or ERK (pERK). As reported previously (Kirilly et al., 2011; Liu et al., 2010; Schultz et al., 2002), pERK is highly expressed in control ISCs (Fig. 6A). By contrast, the *sec5-i*, *sec6-i*, *sec10-i* and *sec15-i* ISCs severely decrease or diminish pERK expression (Fig. 6B-E). These results demonstrate that exocyst components are required in ISCs to maintain high MAPK signaling.

Then, we determined if restoration of MAPK signaling in ISCs could rescue the germ cell differentiation defects caused by *sec* gene knockdown. *rolled* (*rl*) encodes the only MAPK in *Drosophila*, and rl^{SEM} is a constitutively active MAPK mutant independently of EGFR receptor activation (Oellers and Hafen, 1996). The expression of rl^{SEM} in ISCs does not cause any obvious adverse effect on germ cell development compared to the control (Fig. 6F and 6G). Interestingly, the expression of rl^{SEM} in *sec* knockdown ISCs can restore MAPK activity, and can also significantly rescue the germ cell differentiation and ISC loss defects caused by *sec* knockdown (Fig. 6H-M). These results demonstrate that the exocyst is required in ISCs to maintain active MAPK signaling, thereby promoting ISC survival and GSC progeny differentiation.

The exocyst regulates EGFR membrane targeting and signaling

MAPK signaling activity is maintained by EGFR activation in ISCs (Liu et al., 2010; Schultz et al., 2002). As reported previously (Liu et al., 2010), ISC-specific *Egfr* knockdown causes germ cell differentiation defects by two independent RNAi lines (Fig. S4A-C). Interestingly, *Egfr* knockdown in adults also results in the ISC loss; the severity of the ISC loss is also correlated well with that of the germ cell differentiation defects (Fig. S4C'). In addition, we used individual GFP-labeled *Egfr* knockdown ISCs to demonstrate that EGFR signaling is also required to directly maintain ISC cellular processes as the exocyst does (Fig. S5). Although control and $Egfr^{f24}$ heterozygous germaria have similar numbers of CBs, the heterozygous $Egfr^{f24}$ mutation can significantly enhance the germ cell differentiation defects caused by *sec5*, *sec6*, *sec10* and *sec15* knockdown in ISCs, demonstrating that EGFR signaling and the exocyst function synergistically in ISCs to promote GSC progeny differentiation (Fig. 6N-P). Interestingly, EGFR proteins are expressed in speckles in ISCs and follicle progenitor cells, which are greatly decreased in the *c587*-driven *Egfr* knockdown germaria, suggesting that EGFR protein is present in speckles of ISCs and follicle progenitor cells (Fig. S4D-E'). Interestingly, some EGFR-positive speckles are also positive for Sec15-GFP in control ISCs, suggesting that EGFR is localized to Sec15-positive cellular vesicles (Fig. 6Q, 6Q'). These results suggest that the exocyst might regulate EGFR trafficking in ISCs to maintain ISCs and promote GSC progeny differentiation.

In the individual GFP-labeled control ISCs, EGFR protein speckles are localized to the cell body and cellular processes, but are rarely detected on the basal side facing away from germ cells (Fig. 6R, 6R'; Fig. S6A-A"). Similarly, we also detected very few Sec10/15-positive vesicles on the basal side of ISCs (Fig. 2A-2B'). In the individual GFP-labeled *sec5-i*, *sec6-i* or *sec10-i* ISCs, EGFR protein speckles are only present in the cell body due to the loss of cellular processes (Fig. 6S, 6S'; Fig. S6B-D"). In addition, the GFP-labeled *sec* knockdown ISCs also accumulate more EGFR-positive speckles on the basal side. Since EGF ligands responsible for EGFR activation in ISCs are known to come from underneath differentiated germ cells (Liu et al., 2010), our results suggest that the exocyst is required for polarized EGFR-containing vesicle trafficking to cellular processes to maximize EGFR activation by EGF ligands in germ cells, thereby facilitating MAPK signaling.

The exocyst is directly associated with EGFR-carrying vesicles to regulate their membrane trafficking

Previous studies suggest that the human exocyst complex can directly interact with human EGFR in cultured cells (Fogelgren et al., 2014; Tan et al., 2015). Then, we determined if the *Drosophila* exocyst also interacts with EGFR *in vivo* and *in vitro*. Indeed, HA-tagged membrane-associated EGFR intracellular domain can pull down Myc-tagged Sec10 and Flag-tagged Sec15 in S2 cells, indicating that the exocyst is associated with EGFR in S2 cells (Fig. 7A). In addition, bacterially expressed Sec10, but not Sec15, directly interacts with purified EGFR intracellular domain *in vitro*, indicating that the exocyst directly binds to EGFR via Sec10-medated interaction (Fig. 7A').

Moreover, ISC-expressing Sec10-GFP and Sec15-GFP can pull down EGFR protein in ovarian extracts, supporting the *in vivo* association of the exocyst and EGFR (Fig. 7A"). These results indicate that the exocyst complex recognizes EGFR-containing vesicles for membrane targeting by directly interacting with EGFR.

Previous studies have shown that the juxtamembrane domain (JM) is important for EGFR to be localized to the basolateral side of epithelial cells (He et al., 2002; Hobert et al., 1997; Kil et al., 1999). In S2 cells, both Myc-Sec10 and Flag-Sec15 fail to be brought down by the EGFR lacking the JM domain, but can specifically be pulled down by the JM-fused GFP protein (Fig. S7). These results indicate that the exocyst specifically interacts with the JM domain of EGFR, and further suggest that it might be involved in the polarized EGFR trafficking in ISCs.

The exocyst regulates EGFR membrane targeting and recycling to facilitate EGF-induced EGFR phosphorylation in human cells

Since the functions of exocyst components are highly conserved from yeast to human (Schekman, 2010; Wu and Guo, 2015), we then investigated if the exocyst is also required for targeting human EGFR to the plasma membrane in HeLa and 293T cells by applying the retention using selective hooks (RUSH) assay (Boncompain et al., 2012). In the RUSH assay, SBP-GFP-EGFR (human EGFR tagged with EGFP and the streptavidin binding peptide) is normally retained in the ER by Str-KDEL (streptavidin fused to the ER retention signal KDEL); upon biotin addition, SBP-GFP-EGFR is rapidly released by Str-KDEL from the ER and is then trafficked to the plasma membrane via cellular

vesicles (Figure S8; Video 1). In the mock-transfected control HEK293T and HeLa cells, SBP-GFP-EGFR is efficiently trafficked to the cell surface upon biotin addition, but it is still primarily retained inside the *Exoc5KD* and *Exoc6KD* cells (*Exoc5* and *Exoc6* represent *sec 10* and *sec15* in humans, respectively) (Fig. 7B-B"; Fig. S9A-C). Consequently, *Exoc5/6* knockdown cells had significantly less surface GFP-EGFR protein than the control cells (Fig. 7B"; Fig. 9C). In addition, Exoc5 knockdown causes a significant reduction of surface-localized EGFR in Hela cells (Fig. S9D-E). Using an *in vitro* assay that reconstitutes vesicular release of EGFR (Ma et al., 2018) (Fig. 7C), we have further ruled out the possibility that the exocyst regulates the packaging of EGFR into transport vesicles since *Exoc5/6* knockdown does not affect the vesicle-associated EGFR levels in 293T cells (Fig. 7C'). Then, we utilized two-color stochastic optical reconstruction microscopy (STORM), which can achieve a spatial resolution of 20 nm (Zhao et al., 2015), to show that EGFR punctae are spatially overlapped with EEA1 punctae, but not Rab11 and LAMP2 punctae, in *Exoc5* knockdown cells (Fig. 7D-D'). EEA1, Rab11 and LAMP2 label early endosomes, recycling endosomes and lysosomes, respectively. These results indicate that the exocyst is important for the delivery of EGFR protein to the plasma membrane possibly through EEA1-positive early endosomes.

To further determine if the exocyst is required for EGF-induced EGFR endocytosis and recycling, we examined the surface EGFR levels in the control and *Exoc5KD* after EGF stimulation (Fig. S10A, S10D). In both the control and *Exoc5KD* cells, EGFR is co-localized with early endosomal marker EEA1 15 min after EGF stimulation, indicating that Exoc5 is dispensable for EGF-induced EGFR endocytosis

(Fig. S10B, S10C). Interestingly, 60 min after EGF stimulation, EGF-bound EGFR is retrieved back to the plasma membrane or transported to lysosomes for degradation (Fig. S10E). In contrast, *Exoc5KD* cells have much less EGFR on the plasma membrane than the control cells 60 min after EGF stimulation, indicating that Exoc5 is important for the recycling, but not the endocytosis, of EGF-activated EGFR in human cells (Fig. S10F). Then, we utilized the antibodies that specifically recognize the phosphorylated EGFR (pEGFR) to monitor EGFR phosphorylation in the control and *Exoc5KD* HeLa cells based on immunostaining and Western blotting (Fig. 7E-G). Remarkably, EGF-induced EGFR phosphorylation is severely and significantly decreased in the *Exoc5KD* cells compared to that in the control cells (Fig. 7F-F"'). These results demonstrate that Exoc5 is important for EGF-induced EGFR phosphorylation and EGFR recycling, but not endocytosis.

Discussion

Accumulated experimental evidence demonstrates that ISCs function as the niche to prevent BMP signaling and promote GSC progeny differentiation via multiple signaling pathways (Eliazer et al., 2014; Eliazer et al., 2011; Kirilly et al., 2011; Li et al., 2015; Liu et al., 2010; Liu et al., 2015; Lu et al., 2015; Luo et al., 2015; Ma et al., 2014; Maimon et al., 2014; Su et al., 2018; Tseng et al., 2018; Wang et al., 2015; Wang and Page-McCaw, 2018; Wang et al., 2011). In addition, long ISC cellular process-mediated interactions are critical for proper GSC progeny differentiation partly by repressing BMP signaling and also potentially through direct signaling (Banisch et al., 2017; Kirilly et al.,

2011; Lu et al., 2015; Maimon et al., 2014; Su et al., 2018; Tseng et al., 2018). However, it remains largely unclear how ISC long cellular processes and ISC-operating signaling pathways are regulated at the cellular level. This study demonstrates that the exocyst is required in adult ISCs to promote EGFR signaling, prevent BMP signaling and maintain ISCs and cellular processes, thereby promoting GSC progeny differentiation (Fig. 7H). This represents the first *in vivo* study for uncovering the function of the exocyst in stem cell regulation as well as in direct regulation of EGFR membrane trafficking.

This study has provided several significant novel insights into the functions of ISCs as the niche for promoting GSC progeny differentiation. First, this study shows that the exocyst can directly regulate EGFR membrane targeting and signaling in *Drosophila* by Sec10-mediated physical interaction. The exocyst is required in ISCs to sustain ERK signaling activity, contributing to GSC progeny differentiation. EGFR signaling is the only pathway known to maintain active ERK signaling in ISCs (Liu et al., 2010; Schultz et al., 2002). EGFR protein and Sec10/15-GFP are co-localized in cellular vesicles of ISCs. Mechanistically, *Drosophila* EGFR is associated with the exocyst in ISCs and S2 cells via interaction with Sec10. Such direct interaction between the exocyst and EGFR is also conserved in vertebrates (Fogelgren et al., 2014). The exocyst knockdown ISCs randomly accumulate EGFR-positive vesicles throughout the cytoplasm, which is in contrast with the preferential localization of EGFR-carrying vesicles on the apical side of ISCs, suggesting that the exocyst might be important for polarized vesicle trafficking in ISCs. Consistent with the idea, Sec10 and Sec15 physically interact with the juxtamembrane domain (JM) of EGFR, which is known to be important for polarized

EGFR trafficking and localization in mammalian epithelial cells (Hobert et al., 1997). The EGFR-containing cellular vesicles in long cellular processes might help present EGFR for maximizing EGFR signaling activated by germ cell-secreted EGF ligands. This could potentially explain the ERK signaling defect in the exocyst knockdown ISCs mechanistically. Similarly, we have shown that human Exoc5 and Exoc6 are also required for EGFR membrane targeting in human HEK293T and HeLa cells, demonstrating the conserved role of the exocyst in EGFR membrane targeting. Interestingly, in *Exoc5* knockdown human cells, EGFR protein accumulates in EEA1-positive early endosomes, suggesting that early endosomes might also participate in EGFR membrane trafficking. Our findings in *Drosophila* and human cells have further supported the proposal of one recent study that the exocyst complex can first assemble on the surface vesicle and then promote vesicle fusion to the plasma membrane, and have also further suggested that some cargos on the surface of vesicles, such as EGFR, might serve as the anchor for facilitating the assembly of the exocyst complex (Ahmed et al., 2018). Thus, this study has revealed an important role of the exocyst in the regulation of EGFR signaling in ISCs by directly controlling EGFR cell surface trafficking (Fig. 7H).

Second, the exocyst is required in ISCs to promote GSC progeny differentiation partly by preventing BMP signaling. One of the well-defined functions of ISCs in promoting GSC progeny differentiation is to prevent BMP signaling (Eliazer et al., 2014; Eliazer et al., 2011; Kirilly et al., 2011; Liu et al., 2010; Liu et al., 2015; Lu et al., 2015; Ma et al., 2014; Wang et al., 2011). BMP signaling is necessary and sufficient for GSC self-renewal by preventing differentiation via *bam* expression (Chen and McKearin, 2003;

Song et al., 2004; Xie and Spradling, 1998). Interestingly, exocyst knockdown in ISCs causes the elevation of BMP signaling activity in the accumulated SGCs at least partly by upregulating *dpp* expression. Consistently, ISC-specific *dpp* knockdown can partially and significantly rescue the germ cell differentiation defect and the ISC loss caused by exocyst knockdown. These results demonstrate that the exocyst is required in ISCs to promote GSC progeny differentiation partly by preventing BMP signaling. EGFR signaling is required in ISCs to preventing BMP signaling by repressing *dally* expression (Liu et al., 2010). As discussed earlier, the exocyst is required in ISCs to maintain active EGFR signaling. Therefore, the exocyst functions in ISCs to prevent BMP signaling in GSC progeny by repressing *dpp* expression and maintaining EGFR signaling (Fig. 7H). This is in contrast with the previously demonstrated intrinsic requirement of the exocyst for promoting BMP signaling inside GSCs in the *Drosophila* testis (Michel et al., 2011).

Third, the exocyst is required in ISCs to promote GSC progeny differentiation also at least partly by maintaining ISCs and their cellular processes. Our previous studies have demonstrated that ISCs themselves and their cellular processes are critical for GSC progeny differentiation (Kirilly et al., 2011; Lu et al., 2015; Ma et al., 2014; Wang et al., 2015; Wang et al., 2011). In this study, we show that the exocyst is also required for maintaining ISCs by promoting cell proliferation and survival and for maintaining long ISC cellular processes (Fig. 7H). The exocyst has been shown to regulate polarized exocytosis and be important for membrane trafficking within the cell (Bryant et al., 2010; Langevin et al., 2005; Murthy et al., 2003). In this study, we have shown that Sec10-GFP and Sec15-GFP proteins exhibit punctate patterns underneath the apical membrane of

ISCs and in ISC cellular processes, but rarely accumulate on the basal side. These apically targeted cellular vesicles can bring lipid bilayer membranes to the apical side and particularly cellular processes, which could potentially explain the growth and maintenance of ISC cellular processes mechanistically. Consistently, the exocyst knockdown GFP-labeled individual ISCs frequently lose their cellular processes. Taken together, our findings have revealed several novel *in vivo* roles of the exocyst in regulating the function and maintenance of the adult stem cell niche, which represents important progress toward a better understanding of the stem cell lineage differentiation control (Fig. 7H). In the future, it will be of great interest to investigate if the exocyst regulates the function of the adult stem cell niche in mammalian systems.

Materials and Methods

Drosophila stocks and maintenance

The *Drosophila* stocks were maintained at room temperature on standard cornmeal media unless specified. The information of the following stocks are available from http://flybase.org/: *c587*, *PZ1444*, *bam-GFP*, *Dad-lacZ*, *UAS-CD8GFP*, *ptc-lacZ*, *act5C-gal4* and *UAS-rl*^{Sem}. *sec15-GFP* is the GFP protein trap line (Kelso et al., 2004). The *UAS-RNAi* knockdown strains used in this study include: *sec5* (BL27526, TH00421.N), *sec6* (BL27314, TH00648.N), *sec10* (BL27483, TH00390.N), *sec15* (BL27499, TH00651.N), *ptc* (BL28795, TH00660.N), *Egfr* (BL25781, BL31526 and BL31525), *dpp* [Tr0047A (Ni et al., 2008), sh2 (Haley et al., 2010)]. To maximize the RNAi-mediated knockdown effect, newly eclosed flies were cultured at 29℃ for up to 4

weeks before the analysis of ovarian phenotypes. To obtain individual GFP-labeled RNAi knockdown ISCs, *yw hsflp;act>>Stop y+>>gal4-UAS-GFP* flies were crossed with RNAi strains at 18℃, and F1 female flies were heatshocked at 37℃ for 40 min, and cultured at 29℃ for 3 weeks before harvesting their ovaries for the phenotypic analysis as we did previously (Lu et al., 2015).

Immunohistochemistry

For immunohistochemistry, ovaries were dissected, fixed and stained according to the procedures described previously (Xie and Spradling, 1998). The following antibodies were used in this study: monoclonal anti-Hts (1B1, 1:200, DSHB), chicken anti-GFP (1:200, Life Technology), rabbit anti-β-galactosidase (1:8,000, MP Biomedicals), rabbit anti-phosphorylated ERK1/2 (1:200, Cell Signaling Technology), mouse anti-EGFR (1:50, Sigma), rabbit monoclonal anti-Smad3 antibody (pS423/pS425) (1:200, Epitomics), rabbit anti-Sec5 (1:50, Santa Cruz) and rabbit anti-Sec10 (1:50, Santa Cruz). All pictures were taken with Leica SP5 Confocal Microscope and processed with Leica SP5 software. To measure the fluorescence intensity of pERK in the randomly chosen control and knockdown ISCs, all images were taken under the same parameters at the same time, and were quantified using Leica SP5 software. The fluorescence intensity values were normalized to the background.

The immunofluorescence was performed on Hela and 293T cells as previously described (Ma et al., 2018). The commercial antibodies were: mouse anti-EGFR (Santa Cruz, number: sc-101), rabbit anti-EGFR (Proteintech, number: 18986-1-AP-s; RRID:

AB_10596476), goat anti-EEA1 (Santa Cruz, number: sc-6415; RRID:AB_2096822), mouse anti-LAMP2 (DSHB, H4B4; RRID:AB_528129), rabbit anti-phosphorylated EGFR (cell Signaling Technology, number: 3777s; RRID:AB_2096270). To quantify EGFR levels, at least six representative fields, each containing over 15 cells, were taken in each control and *Exoc5KD* experimental group under the identical exposure times and scaling condition. The fluorescence intensities were quantified using ImageJ as follows: 1) A single fixed threshold was manually chosen and applied to all images; 2) Total fluorescence in each field was determined using ImageJ measure functions and normalized to the total number of cells in that field.

BrdU and TUNEL labeling

For BrdU labeling, flies were fed with yeast paste mixed with 10μM BrdU (Sigma) for 3 days before the dissection. The dissected ovaries were fixed with 4%PFA for 15min and washed, and then incubated in DNase I buffer for 5 min, and in 20 units DNase I at 37 °C for 1 h. Then the ovaries were washed, and incubated with rat anti-BrdU monoclonal antibody (rat mAb-BrdU, 1:400, Abcam),The TUNEL labeling was performed using TUNEL Apoptosis Detection Kit (Yeasen) according to the published procedure (Zhu and Xie, 2003).

qRT-PCR on sorted GFP-positive ISCs

For fluorescence-based quantitative real-time PCR (qPCR), the GFP-labeled control and knockdown ISCs were sorted from 400~600 ovaries for each genotype by FACS, and total RNA was extracted using Trizol (Thermo Fischer Scientific). RNA was

amplified using CellAmp^{TM} Whole Transcriptome Amplification Kit (TAKARA), and qPCR was performed to quantify the expression

Co-immunoprecipitation using *Drosophila* ovarian extracts and S2 cells

S2 cells were grown at 25^{o}C in HyClone SFX-Insect Cell Culture Media (Thermo Fisher Scientific). Transfections were performed using X-treme GENE HP (6366546001; Roche) transfection reagent according to the manufacturer's instructions. pAWH-EGFR$^{TM\text{-}ICD}$ (aa808-aa1377; EGFR-PB transmembrane domain and intracellular domain; FlyBase ID: FBpp0071571), pAMW-Sec10 and pAFW-Sec15 plasmids were constructed according to the Gateway Cloning methods (K240020; 11791019; Thermo Fisher Scientific). To construct the HA-tagged juxtamembrane domain deletion EGFR construct (EGFR$^{JM\Delta}$-HA), amino acid sequence LRPSNIGANLCKLRIVKDAELRKGGVLG was removed from pAWH-EGFR$^{TM\text{-}ICD}$. To generate the GFP tagged the JM domain (GFP-EGFR^{JM}), LRPSNIGANLCKLRIVKDAELRKGGVLG was fused to the 3' end of GFP CDS.

For S2 Co-IP experiments, 12 ml S2 cells were transfected with indicated plasmids. For in *vivo* Co-IP experiments, 200 pairs C587 drive UAS-Sec10-GFP, UAS-Sec15-GFP overexpressed ovaries were digested with type II collagenase (50D11833; Worthington), and eggs were filtered and removed. Cells were then lysed with 800μL ice-cold lysis buffer (50mM Tris-HCl, pH 7.5, 150mM NaCl, 0.5% Triton-100, 1mM EDTA, and a mixture of protease inhibitors). The supernatant of the lysates was incubated with 2μg mouse anti-HA (H3663; Sigma) plus 40μL Protein A/G PLUS-Agarose (sc-2003; Santa Cruz) or 25μL GFP-Trap agarose (gta-10; ChromoTek). Agarose were wash and incubated with 5% BSA at 4^{o}C for 1h, and then added to the

lysates. Supernatant-antibody-agarose mix was incubated overnight at 4°C. After 6 times washes with lysis buffer, the bound complexes were eluted with 2× SDS sample buffer and subjected to SDS-PAGE and immunoblotting. Mouse anti-Flag (F1804; Sigma; 1:2000), mouse anti-HA (H3663; Sigma; 1:2000), mouse anti-Myc (M5546; Sigma; 1:2000) or chicken anti-GFP (A10262; Invitrogen; 1:2000) antibodies were used for WB.

in vitro protein binding

The intracellular domain of EGFR (aa865-aa1377; EGFR-PB intracellular domain; FlyBase ID: FBpp0071571) was cloned into the XhoI of pGEX4T1, full-length Sec10 or Sec15 were cloned into the BamHI/NotI of pET32a(+). After induced expression, bacterial was lysed with B-PER™ Bacterial Protein Extraction Reagent (90078; Thermo Fisher Scientific). The inclusion body was dissolved in 15ml 8M Urea (in 1XTBS, pH7.4). The proteins were then dialzsed with Slide-A-Lyzer™ G2 Dialysis Cassettes (88252; Thermo Fisher Scientific) in 5L 1XTBS, pH7.4 for 24-48 hours at 4°C. After the dialysis, proteins were concentrated with Amicon Ultra-2 Centrifugal Filter Unit (UFC201024; Millipore). 10μg GST or GST-EGFR^{ICD} was mixed with 10μg His-Sec10 or His-Sec15 in 500μL buffer A (50mM Tris-HCl, pH 7.5, 150mM NaCl, 0.001% Triton-100) respectively, 40μL Glutathione Agarose (16100; Thermo Fisher Scientific) was added. The protein-agarose mix was incubated at room temperature for 2h with shaking. After 6 times washes with buffer A, the bound complexes were eluted with 40μL 2× SDS sample buffer and subjected to SDS-PAGE and immunoblotting. Rabbit anti-GST (G7781; Sigma; 1:2000) or mouse anti-His (H1029; Sigma; 1:2000) antibodies were used for WB.

RUSH assay in human HeLa and HEK293 cells

EGFR expression constructs were generated by a standard molecular cloning procedure. The DNA fragment encoding E-cadherin within the plasmid Str-KDEL_SBP-EGFP-Ecadherin (Addgene, Plasmid #65286) was replaced with DNA fragment encoding human EGFR (31-1210). HeLa and HEK293T cells were maintained in Dulbecco's Modified Eagle Medium (DMEM) containing 10% fetal bovine serum and 1% penicillin streptomycin mix (Invitrogen). Transfection of siRNA or DNA constructs into HeLa cells or Hek293T cells were performed as described (Guo et al., 2013; Ma et al., 2018). siRNAs against human *Exoc5* and *Exoc6* were purchased from Ribobio. The commercial antibodies rabbit anti-Exoc5 (Proteintech, number 17593-1-AP) and rabbit anti-Exoc6 (Proteintech, number 12723-1-AP) were used to verify knockdown efficiencies using western blotting. Images were acquired with a Zeiss Axioobserver Z1 microscope system or Leica STED TCS SP5 II Confocal Laser Scanning Microscope.

For RUSH (Retention Using Selective Hook) transport assay, HeLa cells or HEK293T cells were transfected with plasmid encoding Str-KDEL and SBP-EGFP-EGFR for 24h. To release the SBP-EGFP-EGFR from the ER, cells were treated with 40μM D-Biotin (Sigma-Aldrich) and 100ng/μL cycloheximide (Sigma-Aldrich) for the indicated time.

STORM imaging

The imaging buffer for two-color STORM was designed for the two dye combination Alexa 647 and Alexa 750 (Zhao et al., 2015). The buffer contained 10% (w/v) glucose, 25mM Tris(2-carboxyethyl) phosphine hydrochloride solution (TCEP, Sigma-Aldrich 646547), 2mM cyclooctatetraene (Sigma-Aldrich 138924), 560 □g/ml glucose oxidase, 40μg/ml catalase, 50mM Tris-Cl pH 8.0, 1mM ascorbic acid and 1mM methyl viologen. The composition of the imaging buffer provided matched and balanced switching characteristics for both dyes (Zhao et al., 2015). The sample was mounted on a customized glass-bottom chamber filled with imaging buffer. After the region of interest was identified, the laser power was increased to 4 kW/cm2 in both channels enabling rapid "blinking" of dye molecules for single molecule detection and localization. The blinking was recorded by an EMCCD at 30Hz for 15,000 to 20,000 frames based on the abundance of proteins. When each frame was captured, the peak finding algorithm recognized the sites of blinking, followed by the fitting algorithm that determined the centroid of each blinking with nanometer accuracy. These centroids were registered to the final super-resolution image. In addition, active sample locking was applied to stabilize the sample with nanometer accuracy in the x-y plane and z-axis during acquisition. Home-build software was used to generate the localization histogram plotting the cross-section of each protein. Colocalizations of the STORM images were performed using the FIJI co-localization Test function. Each super-resolution images utilized for quantification is the image showing the localization patterns of the indicated protein in the whole juxtanuclear area of each individual cell.

Acknowledgements

We would like to thank Developmental Studies Hybridoma Bank and Bloomington *Drosophila* Stock Center for reagents, and the Ni and Xie lab members for comments and discussions. This work was supported by Tsinghua-Peking Joint Center for Life Sciences (Y. M.), the Ministry of Science and Technology of China (No. 2013CB35102, J. N.), the National Natural Science Foundation of China (No. 31371496, J. N.; No. 31871421, Y. G.), Hong Kong Research Grants Council (26100315, 16101116, 16102218, AoE/M-05/12, and C4002-17G, Y. G.), National Institutes of Health (R01HD097664, T. X.), and the Stowers Institute for Medical Research (T. X.).

Author contributions

Conception and design: TX, JN, YG; acquisition of data: YM, RT, YH, DM, PKL, ZY, JW; analysis and interpretation of data: YM, RT, YH, PKL, YG, DM, JN, TX; drafting or revising the article: TX, JN, YG, YM.

References

Ahmed, S.M., Nishida-Fukuda, H., Li, Y., McDonald, W.H., Gradinaru, C.C., and Macara, I.G. (2018). Exocyst dynamics during vesicle tethering and fusion. Nature communications *9*, 5140.

Banisch, T.U., Maimon, I., Dadosh, T., and Gilboa, L. (2017). Escort cells generate a dynamic compartment for germline stem cell differentiation via combined Stat and Erk signalling. Development *144*, 1937-1947.

Bretscher, M.S. (2008). Exocytosis provides the membrane for protrusion, at least in migrating fibroblasts. Nat Rev Mol Cell Biol *9*, 916.

Bryant, D.M., Datta, A., Rodriguez-Fraticelli, A.E., Peranen, J., Martin-Belmonte, F., and Mostov, K.E. (2010). A molecular network for de novo generation of the apical surface and lumen. Nat Cell Biol *12*, 1035-1045.

Chen, D., and McKearin, D. (2003). Dpp signaling silences bam transcription directly to establish asymmetric divisions of germline stem cells. Curr Biol *13*, 1786-1791.

Decotto, E., and Spradling, A.C. (2005). The Drosophila ovarian and testis stem cell niches: similar somatic stem cells and signals. Dev Cell *9*, 501-510.

Eliazer, S., Palacios, V., Wang, Z., Kollipara, R.K., Kittler, R., and Buszczak, M. (2014). Lsd1 restricts the number of germline stem cells by regulating multiple targets in escort cells. PLoS genetics *10*, e1004200.

Eliazer, S., Shalaby, N.A., and Buszczak, M. (2011). Loss of lysine-specific demethylase 1 nonautonomously causes stem cell tumors in the Drosophila ovary. Proc Natl Acad Sci U S A *108*, 7064-7069.

Fogelgren, B., Zuo, X., Buonato, J.M., Vasilyev, A., Baek, J.I., Choi, S.Y., Chacon-Heszele, M.F., Palmyre, A., Polgar, N., Drummond, I., *et al.* (2014). Exocyst Sec10 protects renal tubule cells from injury by EGFR/MAPK activation and effects on endocytosis. American journal of physiology Renal physiology *307*, F1334-1341.

Fu, Z., Geng, C., Wang, H., Yang, Z., Weng, C., Li, H., Deng, L., Liu, L., Liu, N., Ni, J., *et al.* (2015). Twin Promotes the Maintenance and Differentiation of Germline Stem Cell Lineage through Modulation of Multiple Pathways. Cell Rep *13*, 1366-1379.

Fuller, M.T., and Spradling, A.C. (2007). Male and female Drosophila germline stem cells: two versions of immortality. Science *316*, 402-404.

Haley, B., Foys, B., and Levine, M. (2010). Vectors and parameters that enhance the efficacy of RNAi-mediated gene disruption in transgenic Drosophila. Proc Natl Acad Sci U S A *107*, 11435-11440.

Hay, B.A., Wolff, T., and Rubin, G.M. (1994). Expression of baculovirus P35 prevents cell death in Drosophila. Development *120*, 2121-2129.

He, C., Hobert, M., Friend, L., and Carlin, C. (2002). The epidermal growth factor receptor juxtamembrane domain has multiple basolateral plasma membrane localization determinants, including a dominant signal with a polyproline core. J Biol Chem *277*, 38284-38293.

Hobert, M.E., Kil, S.J., Medof, M.E., and Carlin, C.R. (1997). The cytoplasmic juxtamembrane domain of the epidermal growth factor receptor contains a novel autonomous basolateral sorting determinant. J Biol Chem *272*, 32901-32909.
Huang, J., Reilein, A., and Kalderon, D. (2017). Yorkie and Hedgehog independently restrict BMP production in escort cells to permit germline differentiation in the Drosophila ovary. Development *144*, 2584-2594.
Ito, K., Awano, W., Suzuki, K., Hiromi, Y., and Yamamoto, D. (1997). The Drosophila mushroom body is a quadruple structure of clonal units each of which contains a virtually identical set of neurones and glial cells. Development *124*, 761-771.
Jin, Z., Flynt, A.S., and Lai, E.C. (2013). Drosophila piwi mutants exhibit germline stem cell tumors that are sustained by elevated Dpp signaling. Curr Biol *23*, 1442-1448.
Kelso, R.J., Buszczak, M., Quinones, A.T., Castiblanco, C., Mazzalupo, S., and Cooley, L. (2004). Flytrap, a database documenting a GFP protein-trap insertion screen in Drosophila melanogaster. Nucleic Acids Res *32 Database issue*, D418-420.
Kil, S.J., Hobert, M., and Carlin, C. (1999). A leucine-based determinant in the epidermal growth factor receptor juxtamembrane domain is required for the efficient transport of ligand-receptor complexes to lysosomes. J Biol Chem *274*, 3141-3150.
Kirilly, D., Wang, S., and Xie, T. (2011). Self-maintained escort cells form a germline stem cell differentiation niche. Development *138*, 5087-5097.
Langevin, J., Morgan, M.J., Sibarita, J.B., Aresta, S., Murthy, M., Schwarz, T., Camonis, J., and Bellaiche, Y. (2005). Drosophila exocyst components Sec5, Sec6, and Sec15 regulate DE-Cadherin trafficking from recycling endosomes to the plasma membrane. Dev Cell *9*, 365-376.
Li, C., Kan, L., Chen, Y., Zheng, X., Li, W., Zhang, W., Cao, L., Lin, X., Ji, S., Huang, S., *et al.* (2015). Ci antagonizes Hippo signaling in the somatic cells of the ovary to drive germline stem cell differentiation. Cell research *25*, 1152-1170.
Li, L., and Xie, T. (2005). Stem cell niche: structure and function. Annu Rev Cell Dev Biol *21*, 605-631.
Lin, H., and Spradling, A.C. (1993). Germline stem cell division and egg chamber development in transplanted Drosophila germaria. Dev Biol *159*, 140-152.
Lin, H., Yue, L., and Spradling, A.C. (1994). The Drosophila fusome, a germline-specific organelle, contains membrane skeletal proteins and functions in cyst formation. Development *120*, 947-956.
Liu, M., Lim, T.M., and Cai, Y. (2010). The Drosophila female germline stem cell lineage acts to spatially restrict DPP function within the niche. Science signaling *3*, ra57.
Liu, Z., Zhong, G., Chai, P.C., Luo, L., Liu, S., Yang, Y., Baeg, G.H., and Cai, Y. (2015). Coordinated niche-associated signals promote germline homeostasis in the Drosophila ovary. J Cell Biol *211*, 469-484.
Lu, T., Wang, S., Gao, Y., Mao, Y., Yang, Z., Liu, L., Song, X., Ni, J., and Xie, T. (2015). COP9-Hedgehog axis regulates the function of the germline stem cell progeny differentiation niche in the Drosophila ovary. Development *142*, 4242-4252.
Luo, L., Wang, H., Fan, C., Liu, S., and Cai, Y. (2015). Wnt ligands regulate Tkv expression to constrain Dpp activity in the Drosophila ovarian stem cell niche. J Cell Biol *209*, 595-608.

Ma, T., Li, B., Wang, R., Lau, P.K., Huang, Y., Jiang, L., Schekman, R., and Guo, Y. (2018). A mechanism for differential sorting of the planar cell polarity proteins Frizzled6 and Vangl2 at the trans-Golgi network. J Biol Chem *293*, 8410-8427.
Ma, X., Wang, S., Do, T., Song, X., Inaba, M., Nishimoto, Y., Liu, L.P., Gao, Y., Mao, Y., Li, H., *et al.* (2014). Piwi is required in multiple cell types to control germline stem cell lineage development in the Drosophila ovary. PloS one *9*, e90267.
Maimon, I., Popliker, M., and Gilboa, L. (2014). Without children is required for Stat-mediated zfh1 transcription and for germline stem cell differentiation. Development *141*, 2602-2610.
Margolis, J., and Spradling, A. (1995). Identification and behavior of epithelial stem cells in the Drosophila ovary. Development *121*, 3797-3807.
Michel, M., Raabe, I., Kupinski, A.P., Perez-Palencia, R., and Bokel, C. (2011). Local BMP receptor activation at adherens junctions in the Drosophila germline stem cell niche. Nature communications *2*, 415.
Morris, L.X., and Spradling, A.C. (2011). Long-term live imaging provides new insight into stem cell regulation and germline-soma coordination in the Drosophila ovary. Development *138*, 2207-2215.
Morrison, S.J., and Spradling, A.C. (2008). Stem cells and niches: mechanisms that promote stem cell maintenance throughout life. Cell *132*, 598-611.
Mottier-Pavie, V.I., Palacios, V., Eliazer, S., Scoggin, S., and Buszczak, M. (2016). The Wnt pathway limits BMP signaling outside of the germline stem cell niche in Drosophila ovaries. Dev Biol.
Murthy, M., Garza, D., Scheller, R.H., and Schwarz, T.L. (2003). Mutations in the exocyst component Sec5 disrupt neuronal membrane traffic, but neurotransmitter release persists. Neuron *37*, 433-447.
Murthy, M., Ranjan, R., Denef, N., Higashi, M.E., Schupbach, T., and Schwarz, T.L. (2005). Sec6 mutations and the Drosophila exocyst complex. J Cell Sci *118*, 1139-1150.
Ni, J.Q., Markstein, M., Binari, R., Pfeiffer, B., Liu, L.P., Villalta, C., Booker, M., Perkins, L., and Perrimon, N. (2008). Vector and parameters for targeted transgenic RNA interference in Drosophila melanogaster. Nature methods *5*, 49-51.
Oellers, N., and Hafen, E. (1996). Biochemical characterization of rolledSem, an activated form of Drosophila mitogen-activated protein kinase. J Biol Chem *271*, 24939-24944.
Schekman, R. (2010). Charting the secretory pathway in a simple eukaryote. Mol Biol Cell *21*, 3781-3784.
Schultz, C., Wood, C.G., Jones, D.L., Tazuke, S.I., and Fuller, M.T. (2002). Signaling from germ cells mediated by the rhomboid homolog stet organizes encapsulation by somatic support cells. Development *129*, 4523-4534.
Song, X., Call, G.B., Kirilly, D., and Xie, T. (2007). Notch signaling controls germline stem cell niche formation in the Drosophila ovary. Development *134*, 1071-1080.
Song, X., Wong, M.D., Kawase, E., Xi, R., Ding, B.C., McCarthy, J.J., and Xie, T. (2004). Bmp signals from niche cells directly repress transcription of a differentiation-promoting gene, bag of marbles, in germline stem cells in the Drosophila ovary. Development *131*, 1353-1364.
Song, X., Zhu, C.H., Doan, C., and Xie, T. (2002). Germline stem cells anchored by adherens junctions in the Drosophila ovary niches. Science *296*, 1855-1857.

Spradling, A., Fuller, M.T., Braun, R.E., and Yoshida, S. (2011). Germline Stem Cells. Cold Spring Harbor perspectives in biology.
Spradling, A.C. (1993). Developmental Genetics of Oogenesis. In The Development of *Drosophila melanogaster*, M. Bate, Martinez Arias, A., ed. (Cold Spring Harbor: Cold Spring Harbor Laboratory Press), pp. 1-71.
Su, Y.H., Rastegri, E., Kao, S.H., Lai, C.M., Lin, K.Y., Liao, H.Y., Wang, M.H., and Hsu, H.J. (2018). Diet regulates membrane extension and survival of niche escort cells for germline homeostasis via insulin signaling. Development *145*.
Tan, X., Thapa, N., Sun, Y., and Anderson, R.A. (2015). A kinase-independent role for EGF receptor in autophagy initiation. Cell *160*, 145-160.
Tseng, C.Y., Su, Y.H., Yang, S.M., Lin, K.Y., Lai, C.M., Rastegari, E., Amartuvshin, O., Cho, Y., Cai, Y., and Hsu, H.J. (2018). Smad-Independent BMP Signaling in Somatic Cells Limits the Size of the Germline Stem Cell Pool. Stem cell reports *11*, 811-827.
Wang, S., Gao, Y., Song, X., Ma, X., Zhu, X., Mao, Y., Yang, Z., Ni, J., Li, H., Malanowski, K.E., *et al.* (2015). Wnt signaling-mediated redox regulation maintains the germ line stem cell differentiation niche. Elife *4*, e08174.
Wang, X., and Page-McCaw, A. (2018). Wnt6 maintains anterior escort cells as an integral component of the germline stem cell niche. Development *145*.
Wang, X., Pan, L., Wang, S., Zhou, J., McDowell, W., Park, J., Haug, J., Staehling, K., Tang, H., and Xie, T. (2011). Histone H3K9 trimethylase Eggless controls germline stem cell maintenance and differentiation. PLoS genetics *7*, e1002426.
Ward, E.J., Shcherbata, H.R., Reynolds, S.H., Fischer, K.A., Hatfield, S.D., and Ruohola-Baker, H. (2006). Stem cells signal to the niche through the Notch pathway in the Drosophila ovary. Curr Biol *16*, 2352-2358.
Wu, B., and Guo, W. (2015). The Exocyst at a Glance. J Cell Sci *128*, 2957-2964.
Xie, T. (2013). Control of germline stem cell self-renewal and differentiation in the Drosophila ovary: concerted actions of niche signals and intrinsic factors. WIREs Dev Biol *2*, 261-273.
Xie, T., and Spradling, A. (2001). The Drosophila Ovary: An In Vivo Stem Cell System. In Stem Cell Biology, D.R. Marshak, R.L. Gardner, and D. Gottlieb, eds. (Cold Spring Harbor, N.Y.: Cold Spring Harbor Laboratory Press), pp. 129-148.
Xie, T., and Spradling, A.C. (1998). decapentaplegic is essential for the maintenance and division of germline stem cells in the Drosophila ovary. Cell *94*, 251-260.
Xie, T., and Spradling, A.C. (2000). A niche maintaining germ line stem cells in the Drosophila ovary. Science *290*, 328-330.
Zhao, T., Wang, Y., Zhai, Y., Qu, X., Cheng, A., Du, S., and Loy, M.M. (2015). A user-friendly two-color super-resolution localization microscope. Opt Express *23*, 1879-1887.
Zhu, C.H., and Xie, T. (2003). Clonal expansion of ovarian germline stem cells during niche formation in Drosophila. Development *130*, 2579-2588.

Figures

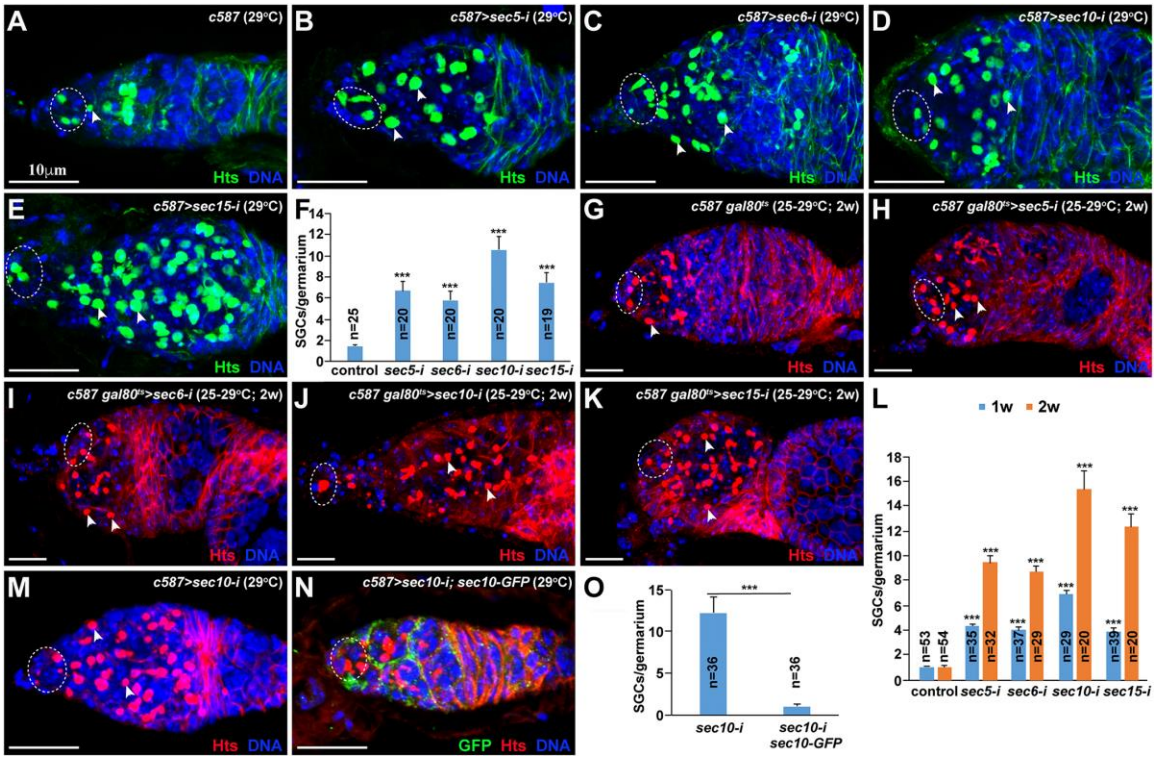

Figure 1. Exocytosis is required in ISCs to promote GSC progeny differentiation. Broken ovals highlight cap cells and GSCs, whereas arrowheads indicate CBs (spectrosome). (**A**) Control germarium contains 3 GSCs and 1 CB. (**B-F**) ISC-specific *sec5/6/10/15-i* germaria carry excess SGCs in addition to normal two or three GSCs. **F**: SGC quantification results (n=the number of the examined germaria; mean±SEM). (**G-L**) Adult ISC-specific *sec5/6/10/15-i* germaria also carry significantly more SGCs than the

control germarium. **L**: SGC quantification results. (**M**-**O**) Sec10-GFP expression in ISCs (**M**) fully suppress the accumulation of SGCs in the *sec10-i* germarium (**N**). **O**: SGC quantification results. All the *P* values in this study are calculated based on the *student's t-test*; *, ** and *** represent <0.05, <0.01 and <0.001, respectively.

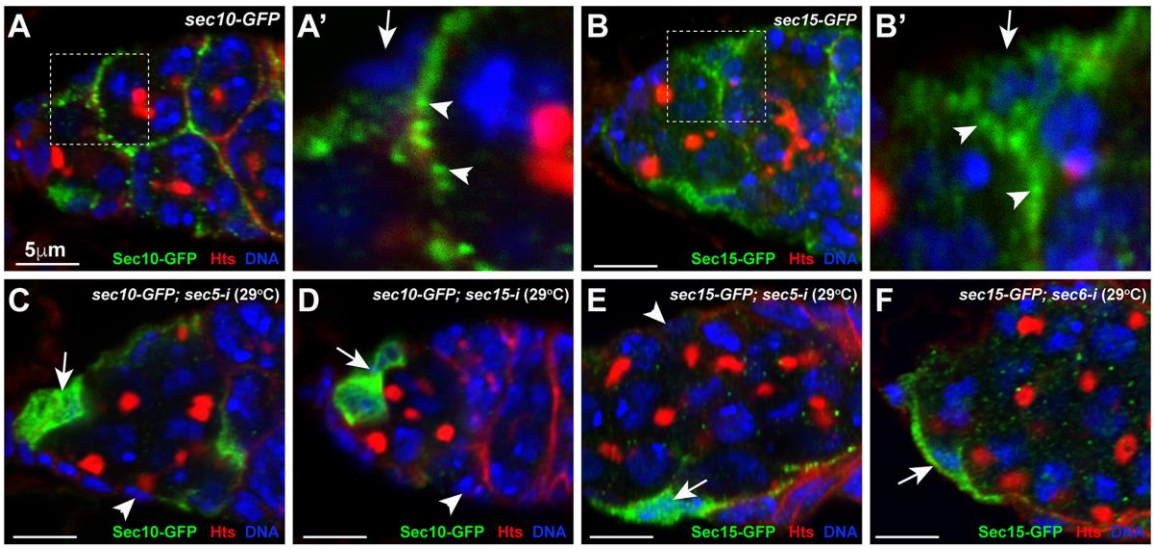

Figure 2. The exocyst complex accumulates on the cellular vesicles at the apical side and in long cellular processes of ISCs. (**A**-**B'**) Sec10-GFP (**A**, **A'**) and Sec15-GFP (**B**, **B'**) accumulate on the cellular vesicles on the apical side (upper arrowhead) and in long cellular processes (bottom arrowhead) of ISCs (arrows indicate the basal side). **A'** and **B'** show the high-magnification views of the highlighted regions in **A** and **B**. (**C**, **D**) *sec5* and *sec15* knockdowns cause uniform Sec10-GFP localization in the cytoplasm of ISCs (arrows) and the loss of Sec10-GFP in some of the knockdown ISCs (arrowheads). (**E**, **F**) *sec5* and *sec6* knockdowns cause uniform Sec15-GFP localization in the cytoplasm of ISCs (arrows) and the loss of Sec15-GFP in some of the knockdown ISCs (arrowhead).

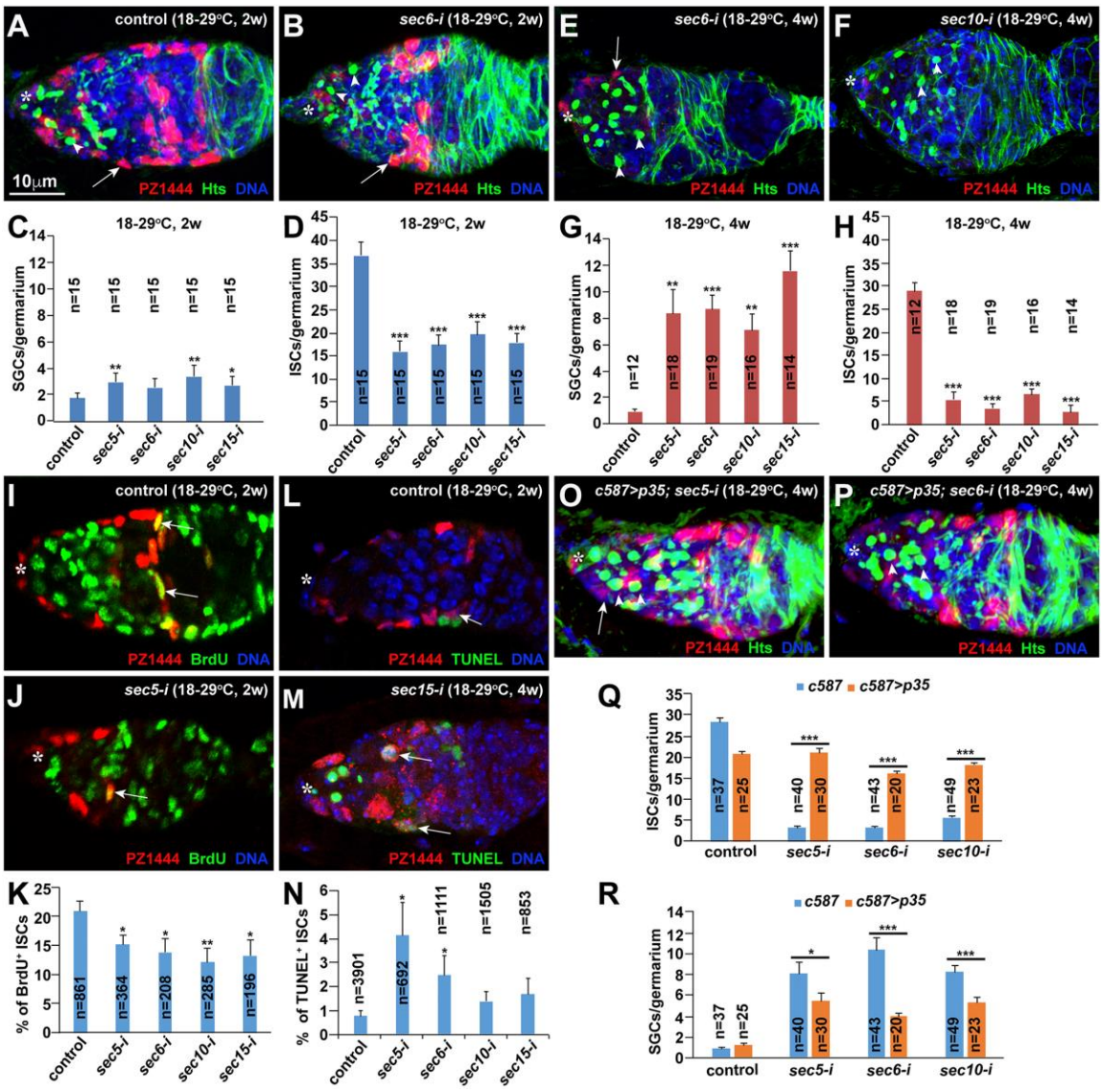

Figure 3. The exocyst complex is required in adult ISCs for their maintenance by promoting cell proliferation and preventing apoptosis. Asterisks highlight the cap cell area, whereas arrows indicate ISCs (**A**, **B**, **E**, **F**, **O**, **P**), proliferating ISCs (**I**, **J**) or apoptotic ISCs (**L**, **M**). (**A-D**) *sec5/6/10/15-i* germaria contain significantly more SGCs and significantly fewer ISCs than the control germaria two weeks after temperature shift

in the adult stage. **C** and **D**: SGC and ISC quantification results. (**E**-**H**) *sec5/6/10/15-i* germaria show more SGCs and fewer ISCs four weeks after the shift than those two weeks after the shift. **G** and **H**: SGC and ISC quantification results. (**I**-**K**) *sec5/6/10/15-i* germaria contain significantly fewer BrdU-labeled ISCs than the control germaria two weeks after the shift. **K**: BrdU-positive ISC quantification results. (**L**-**N**) *sec5/6/10/15-i* germaria carry more apoptotic ISCs than the control germaria two weeks after the shift. **N**: apoptotic ISC quantification results. (**O**-**R**) *p35* expression in ISCs can significantly restore ISCs and rescue the germ cell differentiation defects in *sec5/6/10-i* germaria. **Q** and **R**: SGC and ISC quantification results.

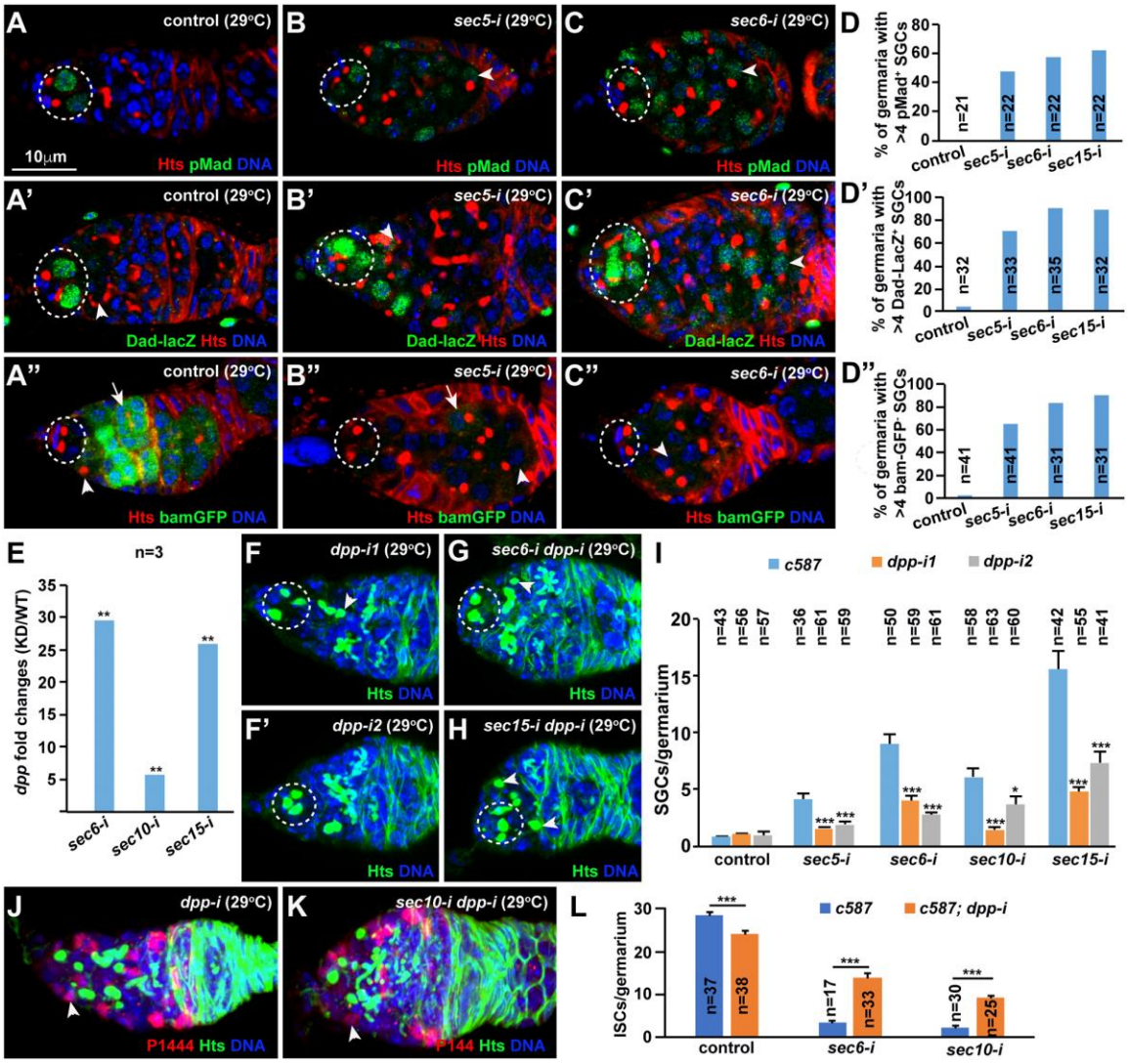

Figure 4. The exocyst is required in ISCs to promote GSC differentiation partly by repressing *dpp* expression. Broken lines highlight GSCs, whereas arrowheads and arrows indicate CBs/SGCs, and cysts, respectively. (**A-D'**) *sec5/6/10/15-i* germaria increase pMad (**B-D**) and *Dad-lacZ* (**B'-D'**) expression in some of the accumulated SGCs in comparison with the controls (**A**, **A'**). (**A"-D"**) *sec5/6/10/15-i* germaria show excess SGCs expressing low *bam-GFP* compared to the CB and cysts in the control. **D-D"**:

quantification results. (**E**) *sec6-i*, *sec10-i* and *sec15-i* ISCs significantly upregulate *dpp* mRNA levels based on quantitative RT-PCR results. (**F-I**) *dpp* knockdown can significantly rescue the germ cell differentiation defect caused by *sec5/6/10/15-i* ISCs. ISC-specific *dpp* knockdown germaria contain one (**F**) or no CB (**F'**). ISC-specific *sec dpp* double knockdown germaria carry one (**G**) or two CBs (**H**). **I**: SGC quantification results. (**J-L**) *dpp* knockdown can significantly rescue the *sec5/6-i* ISC loss (arrow heads indicate ISCs). **L**: ISC quantification results.

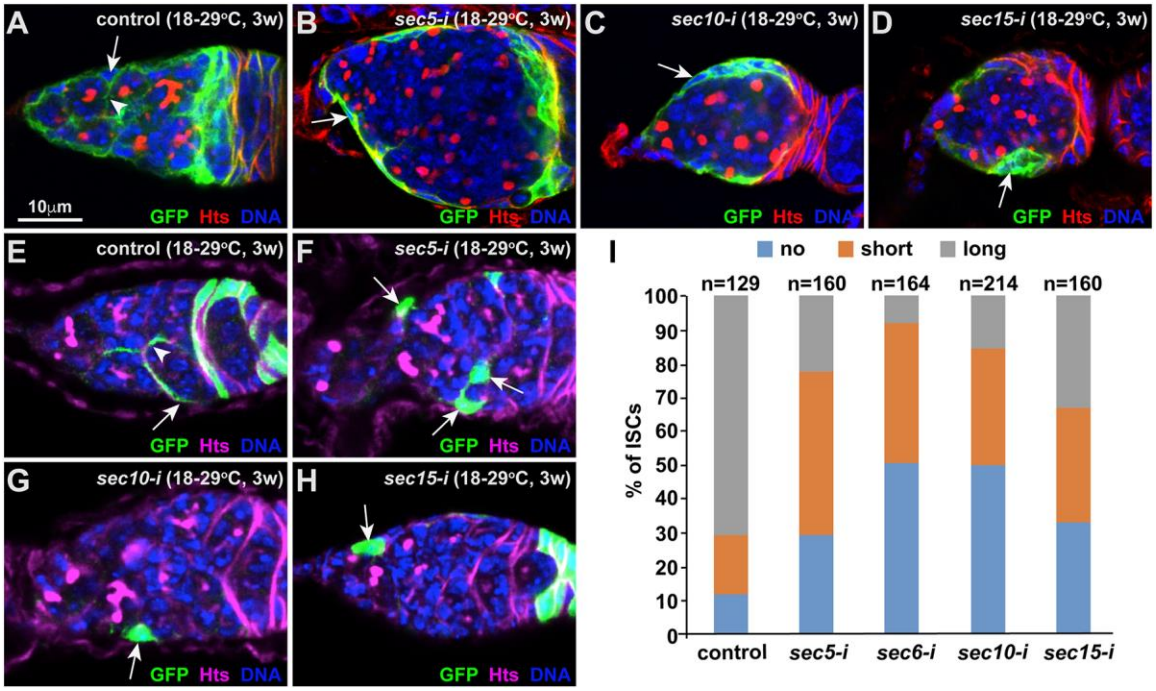

Figure 5. The exocyst is required in ISCs to maintain their cellular processes. Arrows and arrowheads indicate ISCs and their cellular processes, respectively. (**A**-**D**) *sec5/10/15-i* knockdown ISCs (**B**-**D**) lose their long cellular processes wrapping around germ cell cysts in comparison to control (**A**). (**E**-**I**) Individually GFP-marked *sec5*/*6*/*10*/*15-i* ISCs (**F**-**H**) frequently lose their cellular processes compared to the marked control ISCs (**E**). **I**: quantification results on ISC cellular processes based on their length.

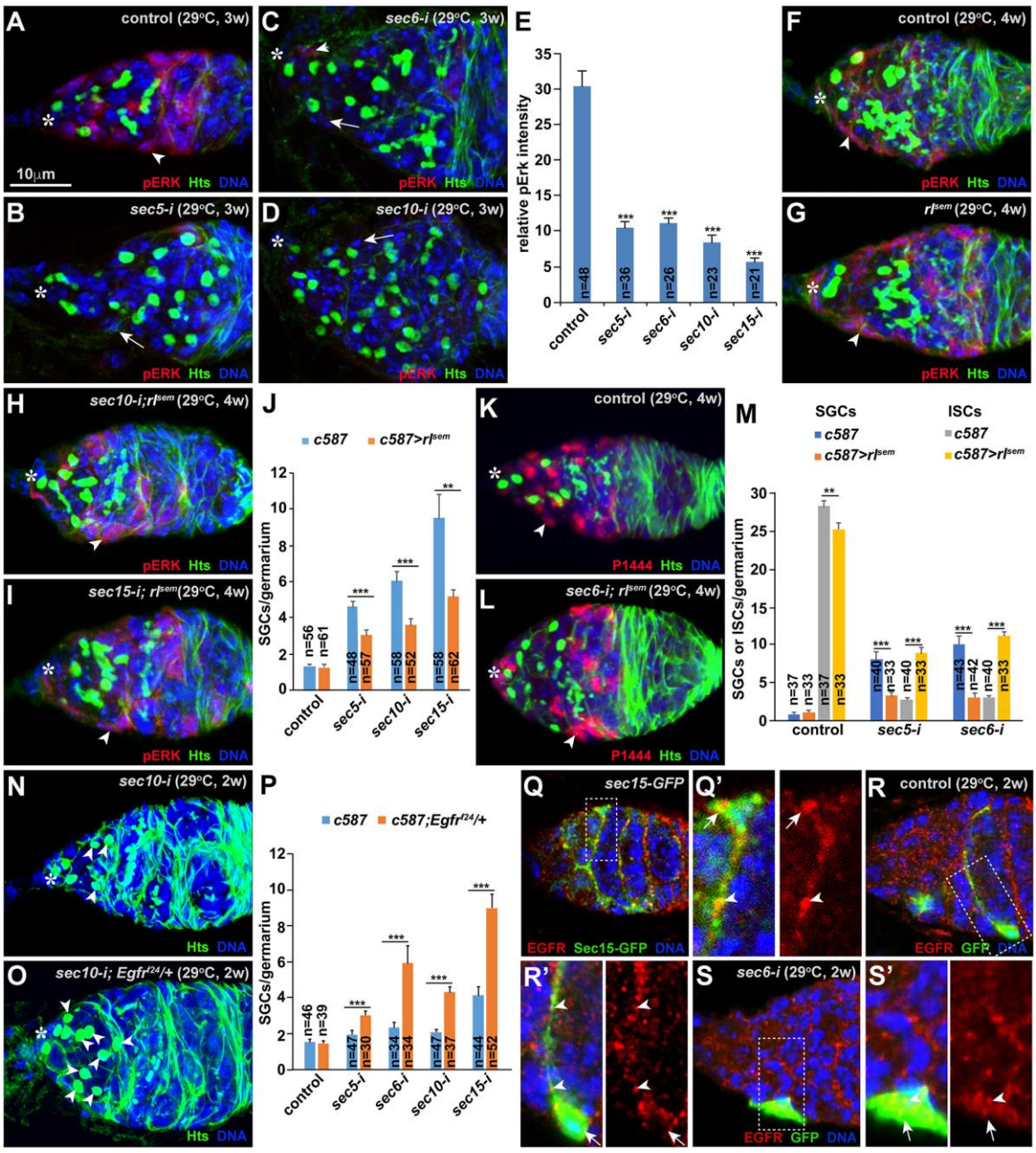

Figure 6. The exocyst is required in ISCs to maintain pERK expression. Asterisks highlight cap cells. (**A-E**) *sec5/6/10/15-i* ISCs (arrowheads) drastically decrease pERK expression in comparison with the control ISC (arrowhead). **E**: quantification results on relative fluorescence intensity. (**F-J**) Expressing constitutively active MAPK (rl^{sem}) can

restore pERK expression in ISCs (arrowheads) in comparison with the wild-type control ISCs (arrowheads), and can also partially and yet significantly rescue the germ cell differentiation defect caused by *sec5/6/10/15-i* in ISCs. **J**: SGC quantification results. (**K-M**) ISC-specific rl^{SEM} expression can significantly rescue the germ cell differentiation and ISC loss defect and the ISC loss caused by *sec5/6-i* (arrowheads indicate ISCs). **M**: SGC and ISC quantification results. (**N-P**) A heterozygous mutation in *Egfr* can significantly enhance the germ cell differentiation defect caused by *sec5/6/10/15-i* based on the accumulation of SGCs (arrowheads). **P**: SGC quantification results. (**Q, Q'**) EGFR protein is localized to the Sec15-GFP-positive vesicles on the apical side of the cell body (arrows) and cellular processes (arrowheads). (**R**, **R'**) A GFP-marked control ISC exhibits EGFR-positive speckles (arrowheads) moving along its cellular process. (**S**, **S'**) A GFP-marked *sec6-i* ISC (arrow) loses its cellular processes, and retain EGFR-positive speckles (arrows) on the basal side (indicated by an arrow).

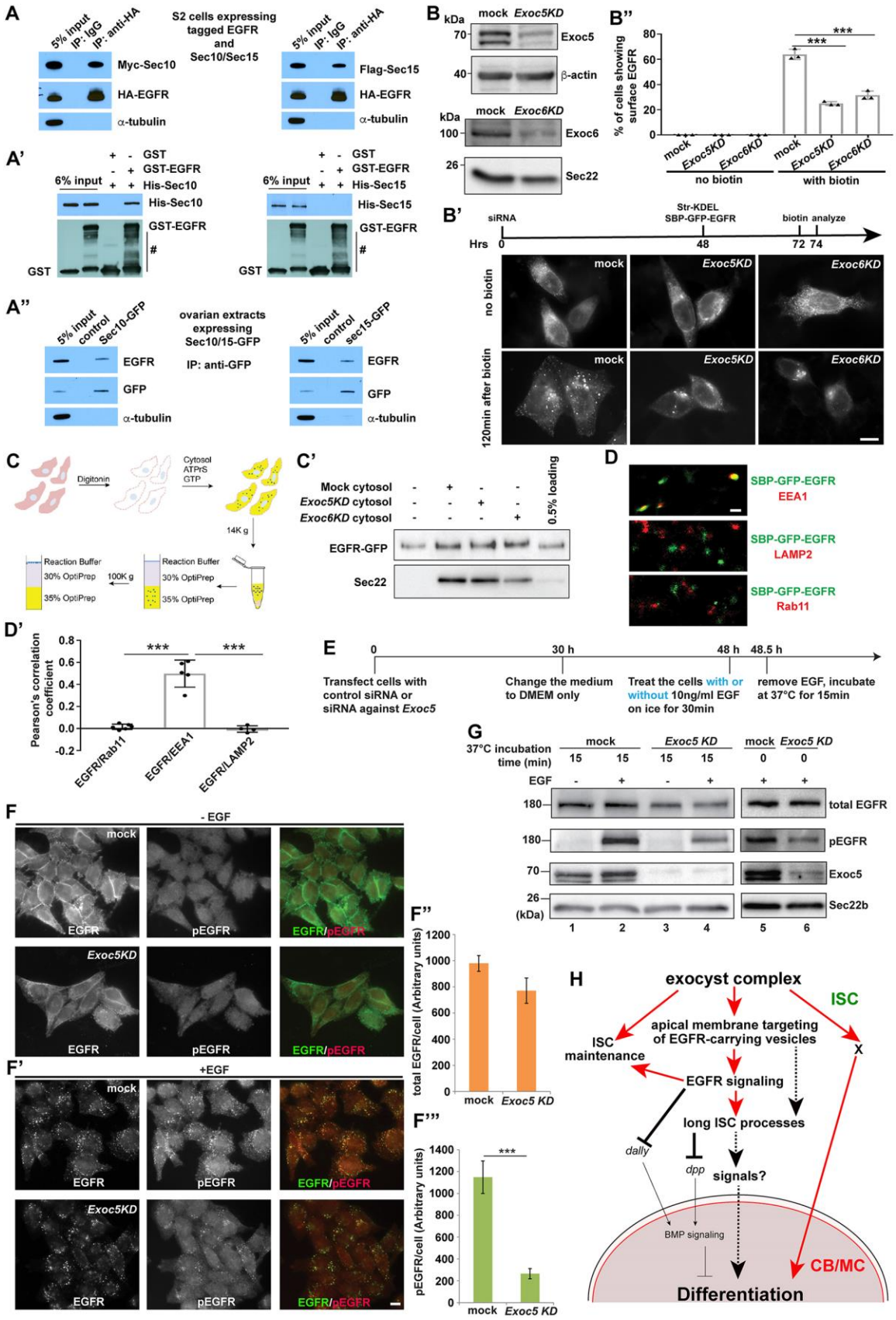

Figure 7. The exocyst is directly associated with EGFR to regulate its membrane targeting in *Drosophila* ISCs and human cells. (**A**-**A”**) HA-EGFR can pull down Myc-Myc-Sec10 and Flag-Sec15 in S2 cells (**A**), but bacterially expressed GST-EGFR can only pull down His-Sec10, but not His-Sec15, *in vitro* (**A’**; # indicate the degraded GST-EGFR). In ovarian extracts, both Sec10-GFP and Sec15-GFP can pull down EGFR protein (**A”**). α-tubulin is used in **A** and **A”** as a negative control. (**B**-**B”**) *Exoc5/6* knockdown (*Exoc5KD* and *Exoc6KD*) significantly decrease the efficiency of delivery of SBP-GFP-EGFR to the plasma membrane. In *Exoc5/6* knockdown Hela cells (**B’**), in which knockdown efficiencies are confirmed by western blots (**B**), SBP-GFP-EGFR remains localized in the perinuclear puncta in contrast to the mock-transfected cells showing detectable surface-localized SBP-GFP-EGFR. **B”**: quantification results on percentage of cells showing detectable cell surface-localized SBP-GFP-EGFR (mean ± S.D.; n = 3; >50 cells counted for each experiment). (**C, C’**) The levels of EGFR-GFP in the vesicle fraction are determined by western blots (**C’**; Sec22 is a cargo protein enriched in vesicles serving as an internal control) after performing the vesicle budding assay described in **C**. (**D, D’**) STORM images show that EGFR-GFP punctae are largely overlapped with EEA1 punctae, but not Rab11 and LAMP2 punctae. D’: quantification results. (**E**-**G**) Exoc5 is required for EGF-induced EGFR phosphorylation (pEGFR; immunostaining in **F** and **F’** and Western blot in **G**) by promoting EGF membrane targeting (**F**) but not endocytosis (**F’**) using the experimental strategy (**E**) (**F”** and **F’”**: quantification results). Bars in **B’**, **D** and **F**: 10μm, 0.5μm and 10μm, respectively. (**H**) A

model showing that the exocyst regulates ISC maintenance, their cellular processes and thus BMP signaling and GSC progeny differentiation by controlling EGFR membrane targeting and other undefined pathways (X) (red arrows represent the relationships revealed by this study).

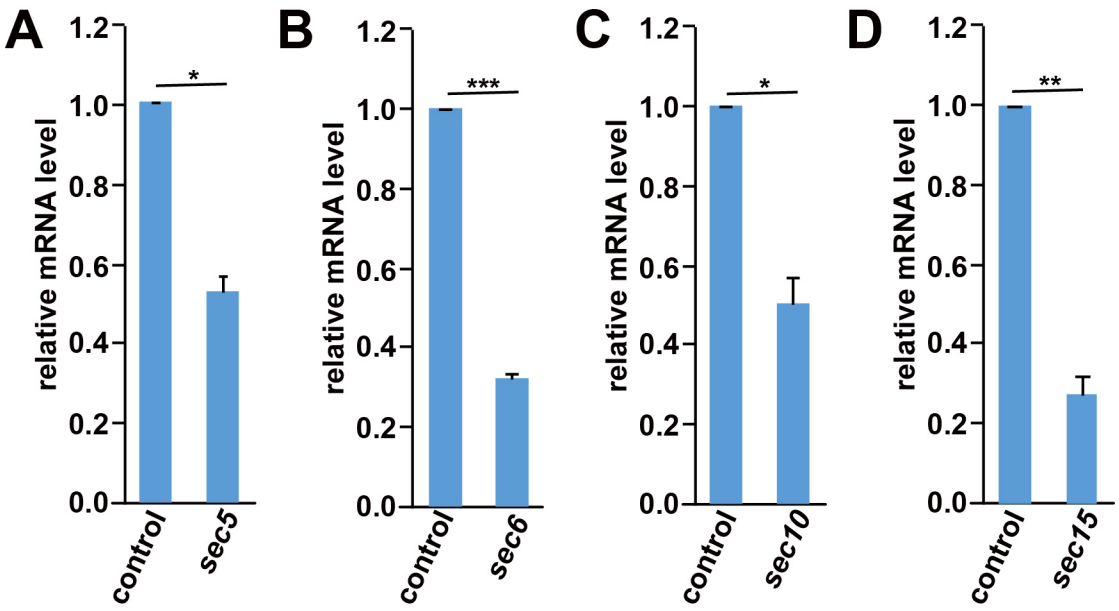

Figure S1. The expression of *sec5/6/10/15* genes can be efficiently knocked down in the ovary by corresponding RNAi lines. (**A**-**D**) Quantitative RT-PCR results show that *actin5C-gal4*-mediated expression of the *UAS-RNAi* lines against *sec5*, *sec6*, *sec10* and *sec15* can significantly knock down their corresponding RNA targets in the isolated germaria (three replicates).

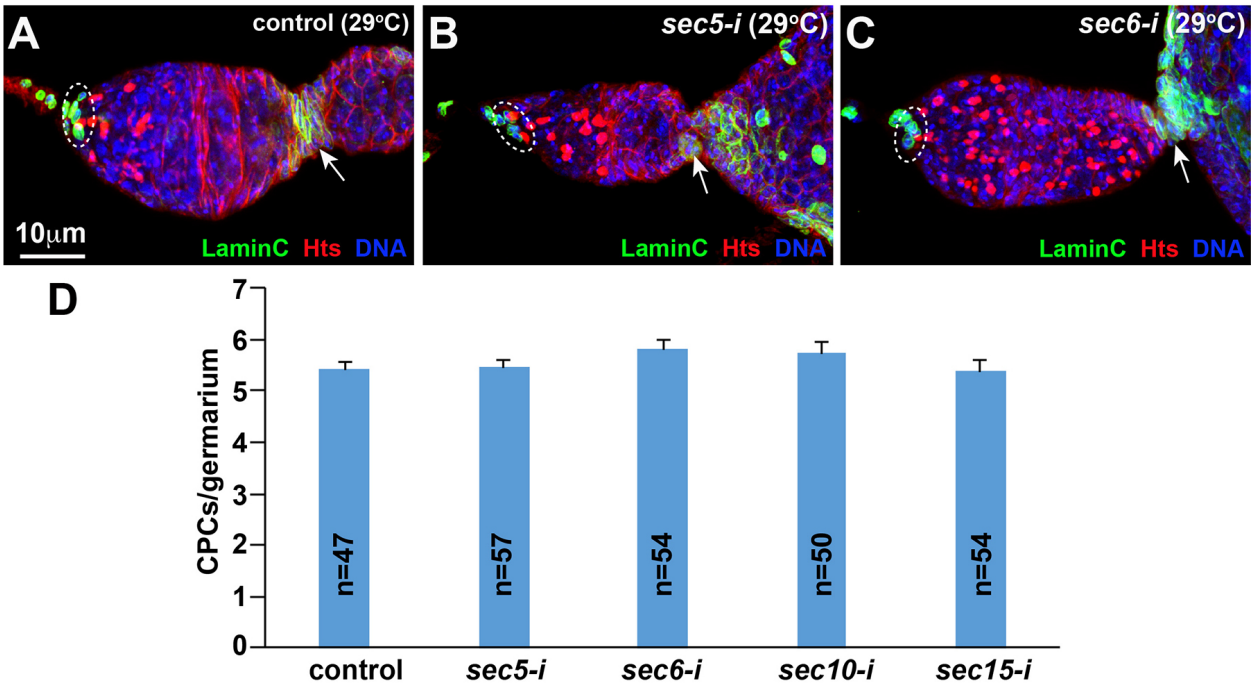

Figure S2. *sec5/6/10/15* knockdown does not convert ISCs into cap cells. Broken ovals highlight Lamin C-positive cap cells and spectrosome-containing GSCs, whereas arrows indicate Lamin C-positive stalk cells. (**A**-**C**) *c587-gal4*-mediated *sec5/6-i* do not change cap cell numbers or convert ISCs to cap cells based on Lamin C expression compared to control (**A**). (**D**) Qualification results show that *sec5/6/10/15* knockdown in ISCs do not change cap cell numbers in comparison to the control.

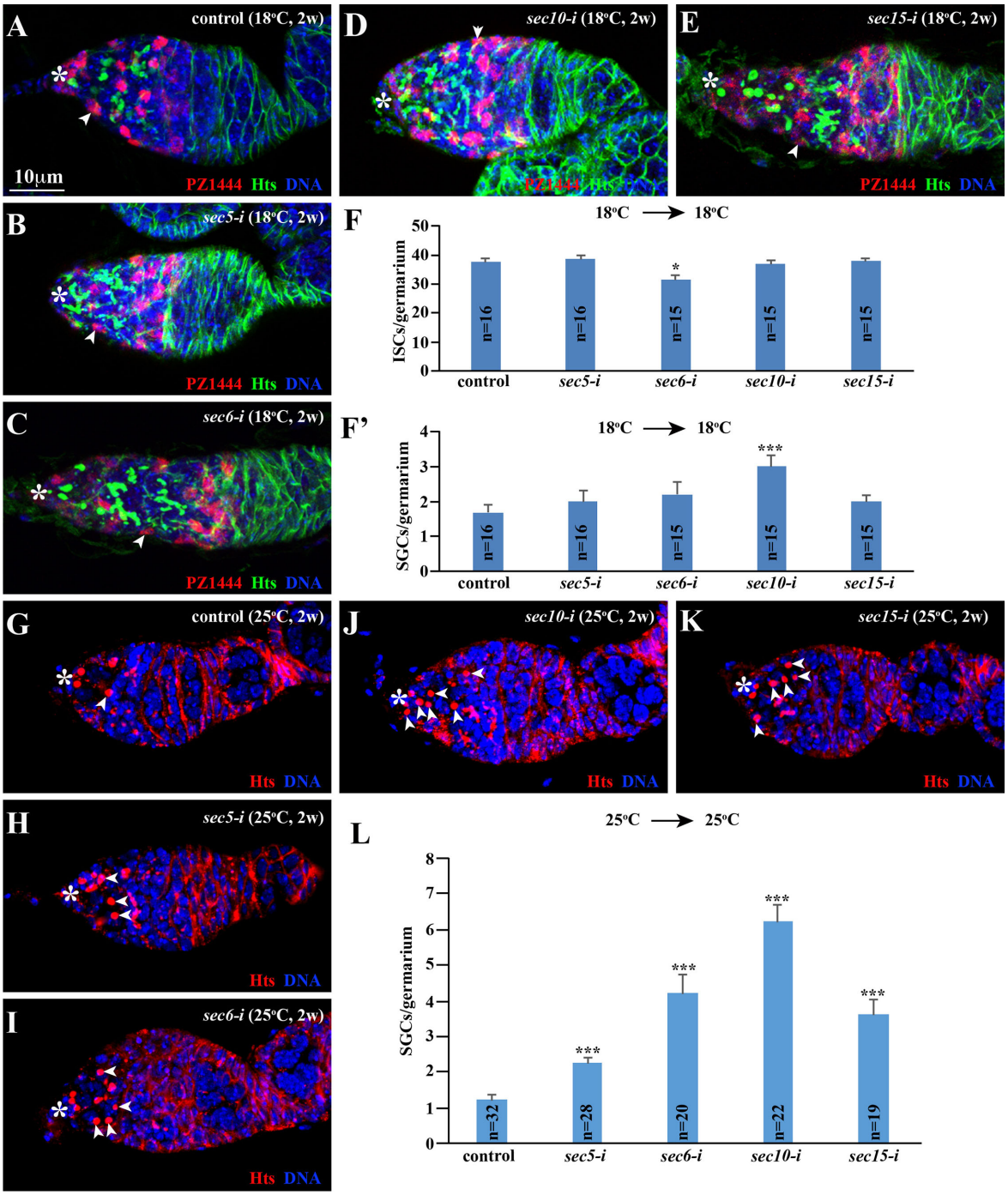

Figure S3. *c587*-driven RNAi knockdown of *sec* genes at 18°C show no effect on the numbers of ISCs, GSCs and CBs. (**A-F'**) *sec5/6/10/15-i* germaria have the normal numbers of ISCs and SGCs in comparison to the control at 18°C. **F** and **F'**: SGC and ISC quantification results, respectively. Asterisks highlight the cap cell area, whereas arrowheads indicate ISCs. (**G-L**) *sec5/6/10/15-i* germaria exhibit a significant increase in the SGC number compared to the control when those *c587;tub-gal80^{ts}*-mediated knockdown females are cultured at 25°C. **L**: SGC quantification results. Asterisks highlight the cap cell area, whereas arrowheads indicate SGCs.

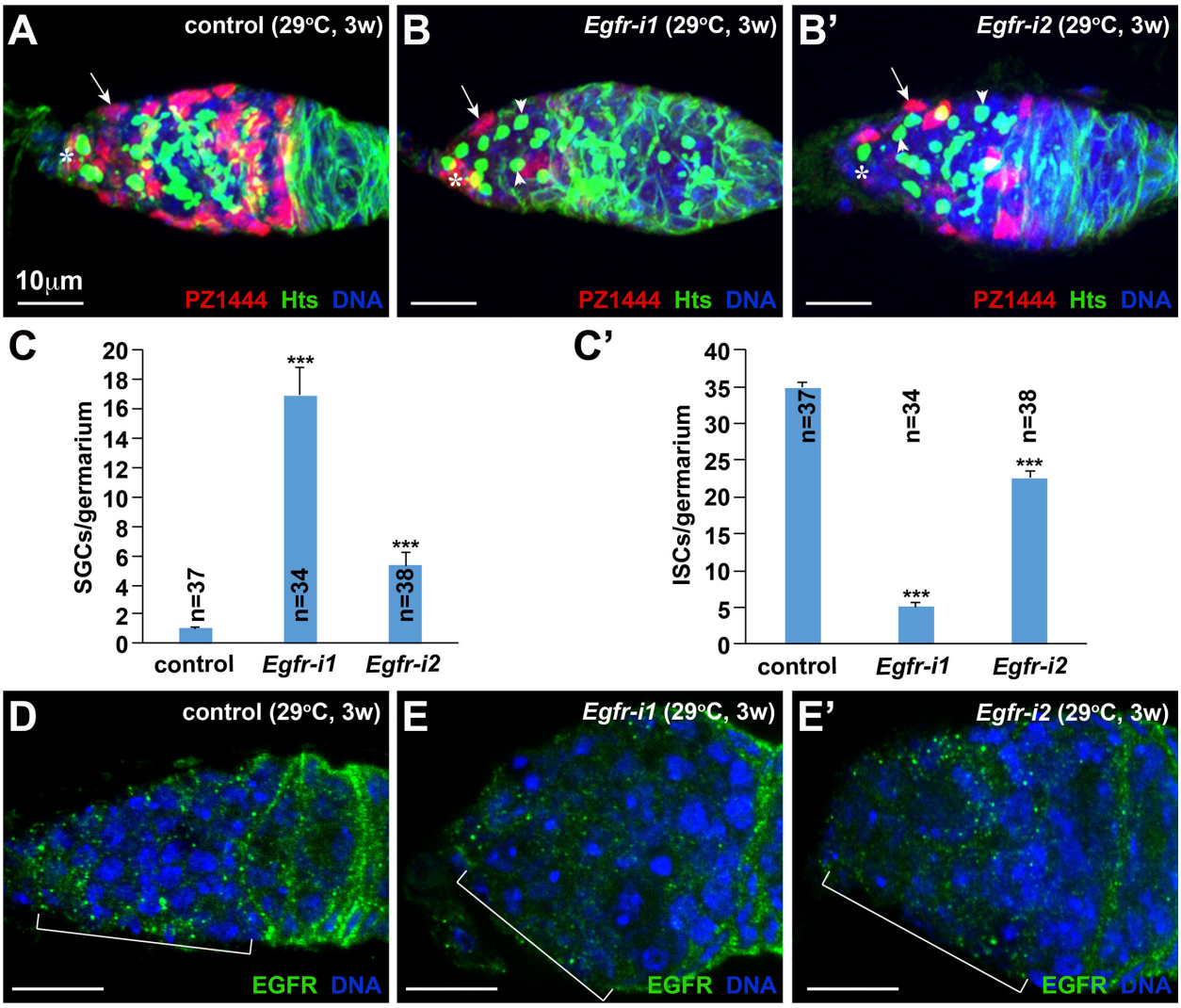

Figure S4. The exocyst complex is required for maintaining ISCs and promoting GSC progeny differentiation. (**A-C'**) *Egfr-i* germaria (**B**, **B'**) contain significantly more SGCs and significantly fewer ISCs than the control germarium (**A**) three weeks after temperature shift to 29°C in the adult stage. **C** and **C'**: SGC and ISC quantification results. Arrows point to ISCs, whereas arrowheads denote spectrosomes. (**D-E'**) EGFR-positive speckles are drastically decreased in the knockdown germaria by two independent RNAi lines (**E**, **E'**) in comparison with the control germarium (**D**).

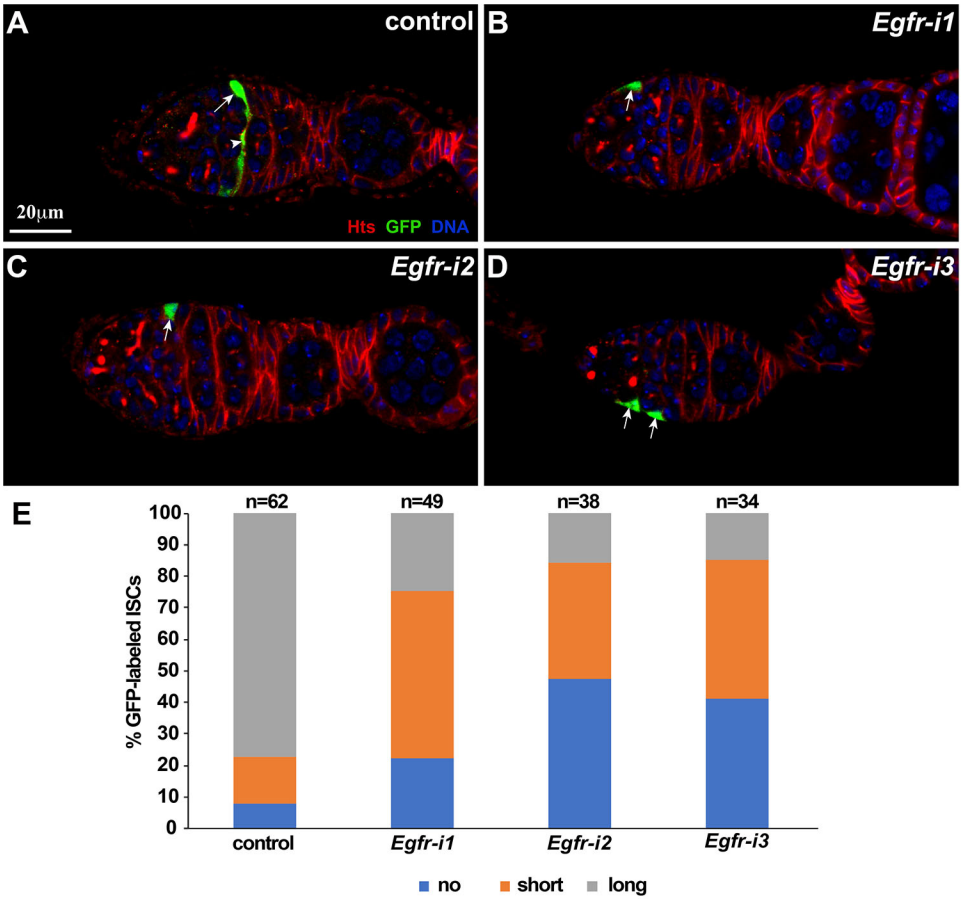

Figure S5. EGFR is required intrinsically for maintaining ISC cellular processes. Arrows and arrowheads indicate ISCs and their cellular processes, respectively. (**A-D**) Individually GFP-marked *Egfr* knock down ISCs by three independent RNAi lines (**B-D**) frequently lose their cellular processes compared to the marked control ISCs (**A**). **E**: quantification results on ISC cellular processes based on their length.

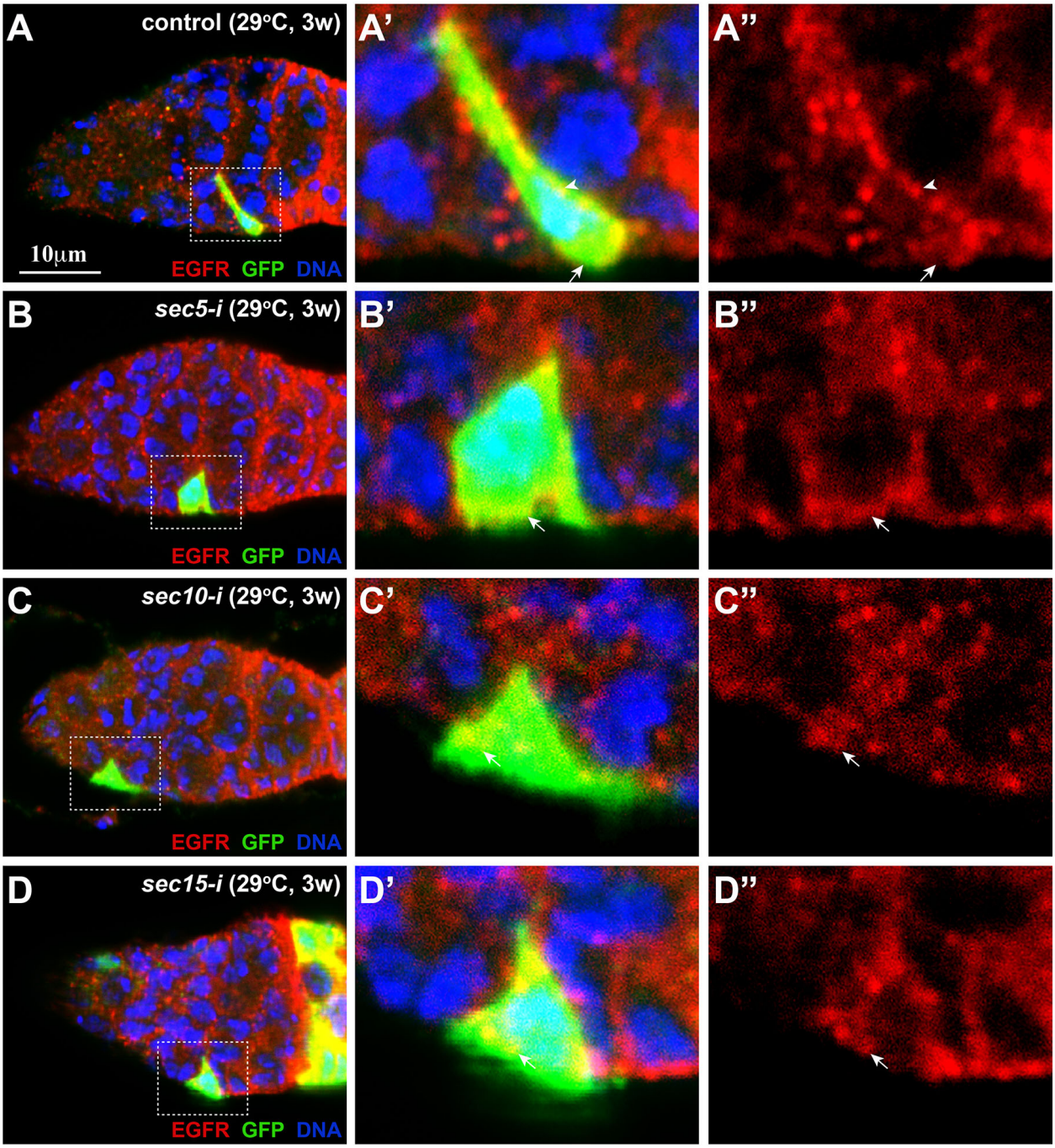

Figure S6. The exocyst is required for the apical trafficking of EGFR protein in ISCs. **A'-D'** and **A"-D"** are highlighted areas in **A-D** at a higher magnification. (**A-A"**) In the control GFP-labeled ISC, EGFR-positive speckles (arrowheads) move along the GFP-labeled ISC cellular process on the apical side, but very few EGFR-positive speckles are observed on the basal side (arrow). (**B-D"**) Individual GFP-marked *sec5-i* (**B-B"**), *sec10-i* (**C-C"**) and *sec15-i* (**D-D"**) ISCs lose their cellular processes, and retain EGFR-positive speckles (arrows, **B'-D'** and **B"-D"**) on both the apical and basal sides.

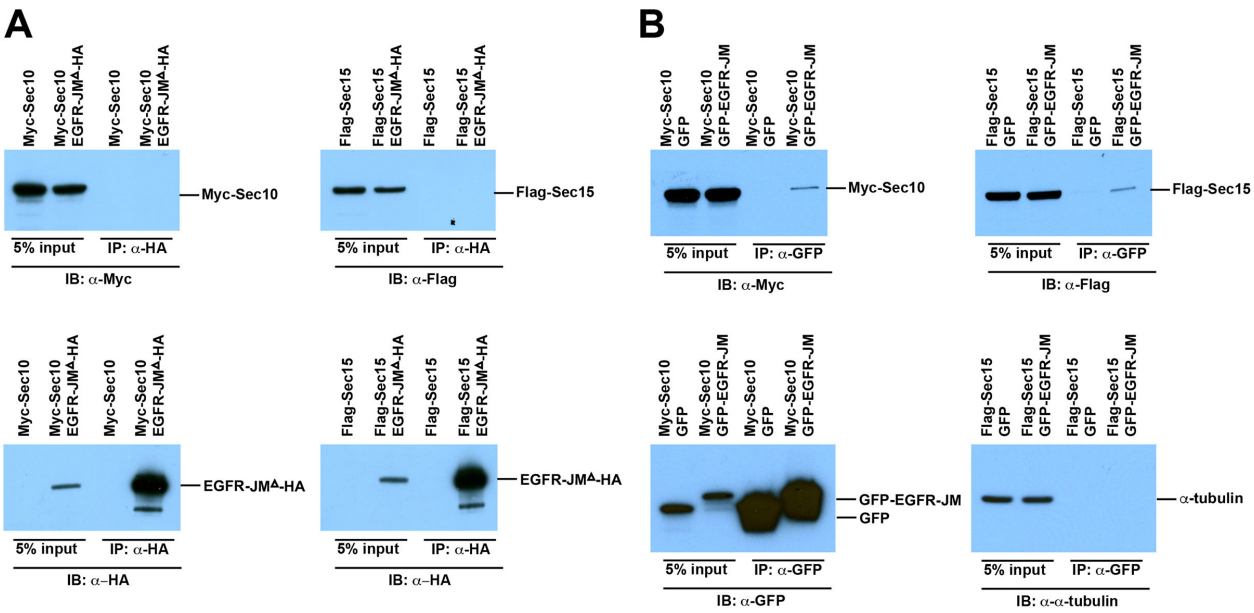

Figure S7. Sec10 and Sec15 are associated with EGFR primarily through binding to the previously defined juxtamembrane domain (JM). (**A**) CO-IP results show that Myc-Sec10 and Flag-Sec15 fail to be brought down by HA-tagged EGFR lacking the JM domain (EGFR-JM$^{\Delta}$-HA) in S2 cells. (**B**) CO-IP results show that Myc-Sec10 and Flag-Sec15 can specifically be pulled down by GFP-tagged the EGFR's JM domain (GFP-MT), but not GFP alone, in S2 cells. α-tubulin is used as a negative control.

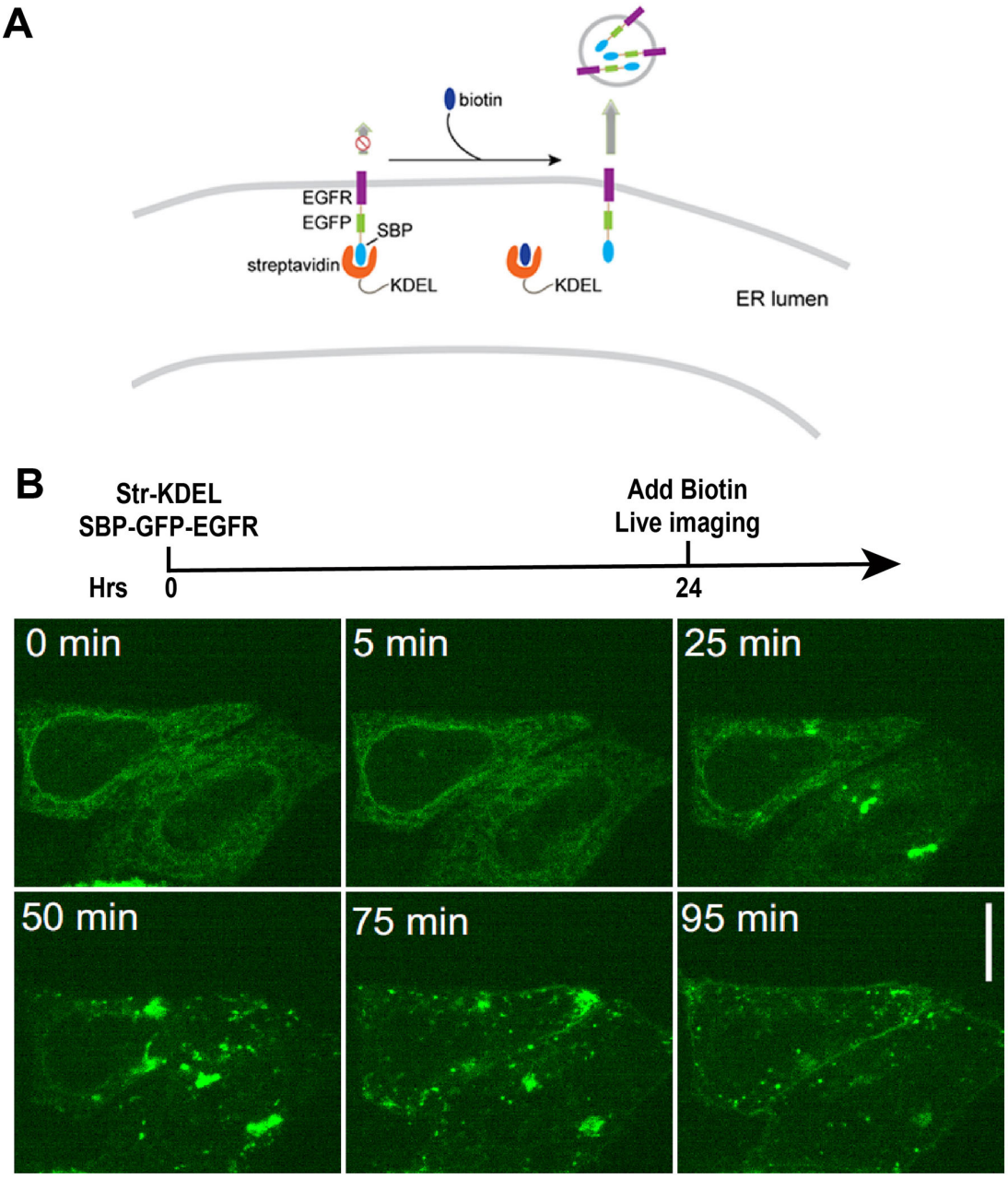

Figure S8. The RUSH transport assay in human cells. (**A**) A diagram explaining the RUSH assay: the binding of streptavidin to SBP causes SBP-GFP-EGFR to be retained at the ER; biotin addition releases streptavidin from SBP-GFP-EGFR to allow SBP-GFP-EGFR for trafficking to the plasma membrane. (**B**) A time-lapse series of confocal images of SBP-GFP-EGFR in Str-KDEL- and SBP-GFP-EGFR-expressing HeLa cells following biotin addition. Confocal images were taken at an interval of 30 seconds following biotin treatment. Representative images at selected time points are shown. Scale bar: 10μm.

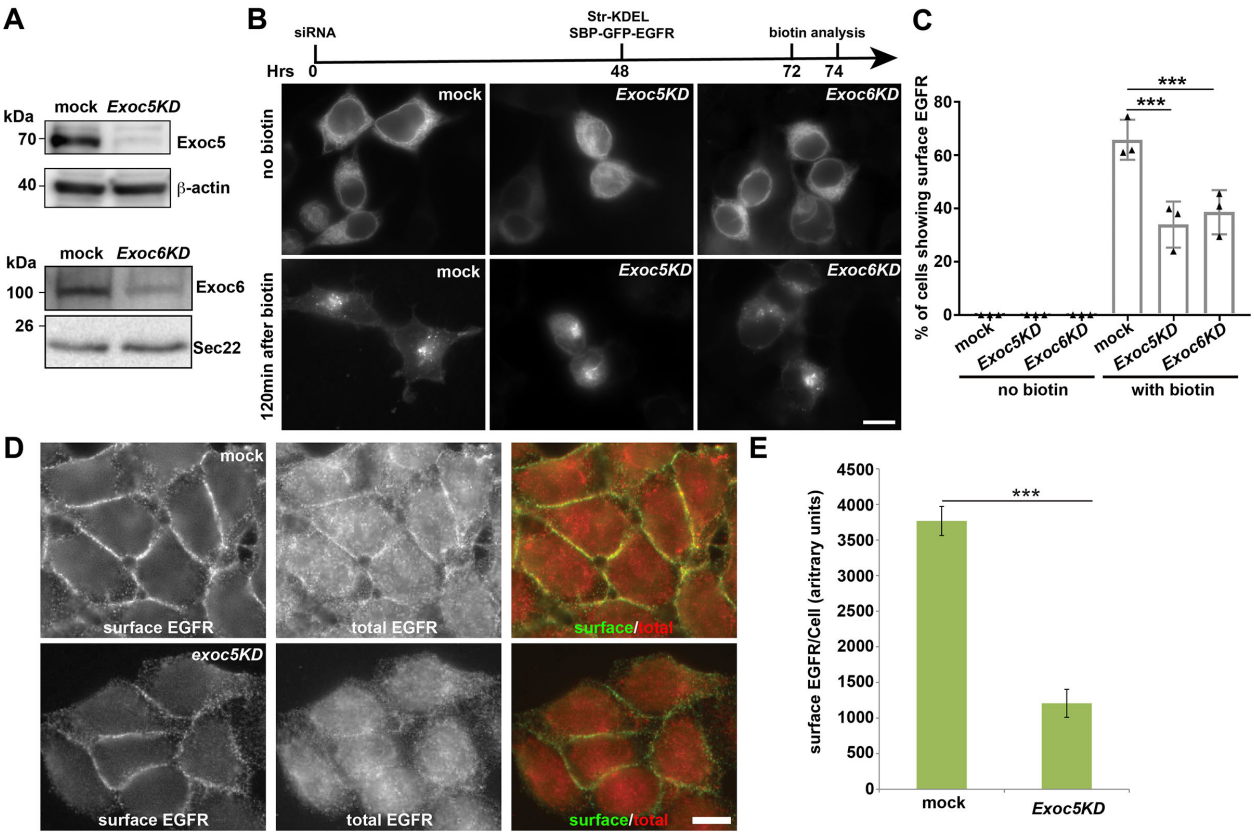

Figure S9. Exoc5 and Exoc6 regulate the surface delivery of newly synthesized EGFR in HEK293T cells. (**A**) Western blots show that siRNAs against *Exoc5* (*Exoc5KD*) and *Exoc6* (*Exoc6KD*) can efficiently knock down the expression of Exoc5 and Exoc6 in HEK293T cells, respectively, compared to the mock transfection. (**B**) *Exoc5KD* and *Exoc6KD* HEK293T cells frequently accumulate SBP-GFP-EGFR in the perinuclear puncta while mock-transfected cells efficiently transported SBP-GFP-EGFR to the plasma membrane. Scale bar: 10μm. (**C**) Quantification results on the percentage of cells showing detectable surface-localized EGFR-GFP in the cells treated with control siRNA, siRNA against *Exoc5* and *Exoc6* (mean ± S.D.; n = 3; >100 cells counted for each experiment). (**D**) *Exoc5KD* HeLa cells show a lower ratio of surface EGFR versus total EGFR than the mock-transfected cells. Scale bar: 10μm. (**E**) Quantification of the average fluorescent levels of the surface EGFR/cell (mean ± SEM; based on seven random fields of images in each experimental group; >15 cells in each field).

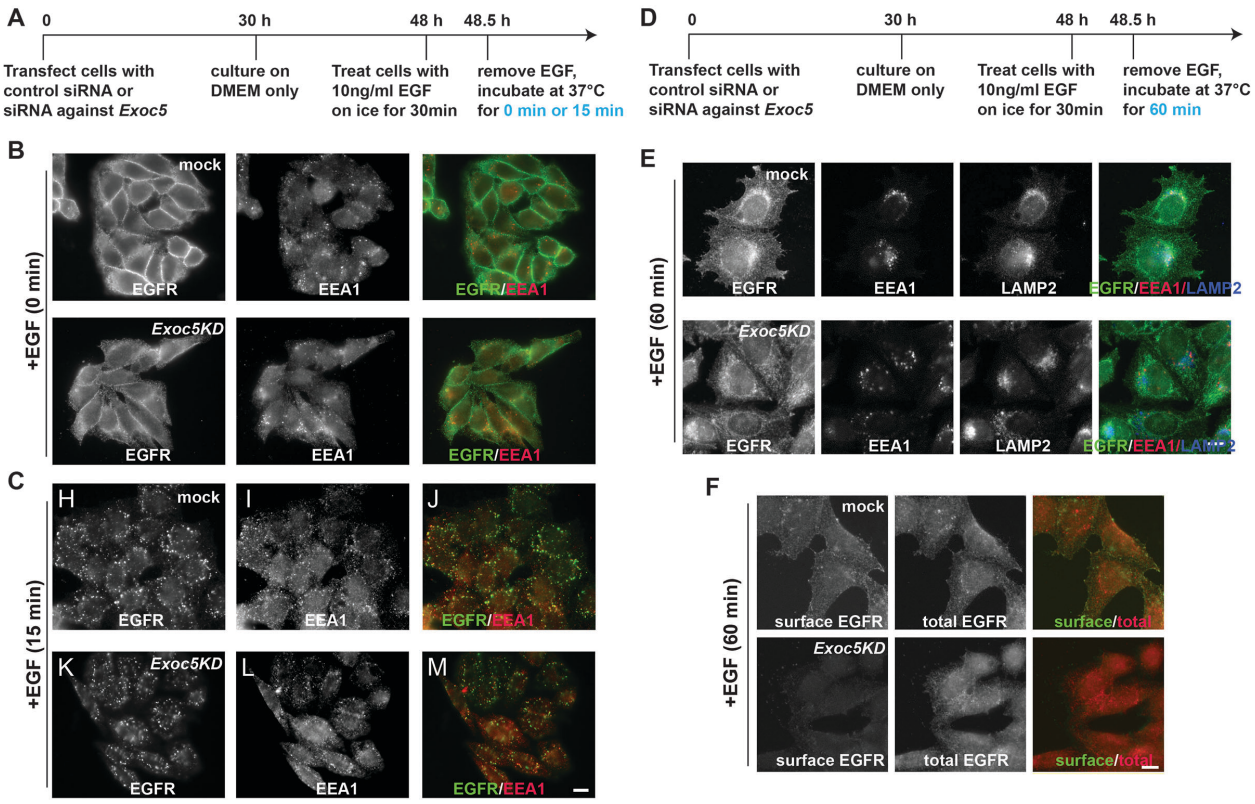

Figure S10. Exco5 is required for the retrieval of internalized EGFR to the plasma membrane, but not for the EGF-induced EGFR endocytosis. (**A-C**) Using the experimental procedures (**A**), *Exoc5* knockdown HeLa cells show lower EGFR on the membrane than control cells after incubation with EGF on ice for 30 min (preventing endocytosis) (**B**). After incubation with EGF on ice for 30min followed by incubation at 37 °C for 15min (initiating EGF activation), EGFR can be endocytosed in both the knockdown and control cells based on EGFR and EEA1 co-localization (**C**). (**D-F**) Using the experimental procedures (**D**), *Exoc5* knockdown HeLa cells exhibit the obvious defect in the EGFR membrane recycling after EGF stimulation in comparison with the control (**E**). Consistently, *Exoc5* knockdown HeLa cells show much less membrane EGFR than the control cells in the presence of the lysosomal enzyme inhibitor, bafilomycin-A1, after EGF stimulation based on surface and total EGFR staining (**F**). Scale bars: 10μm.

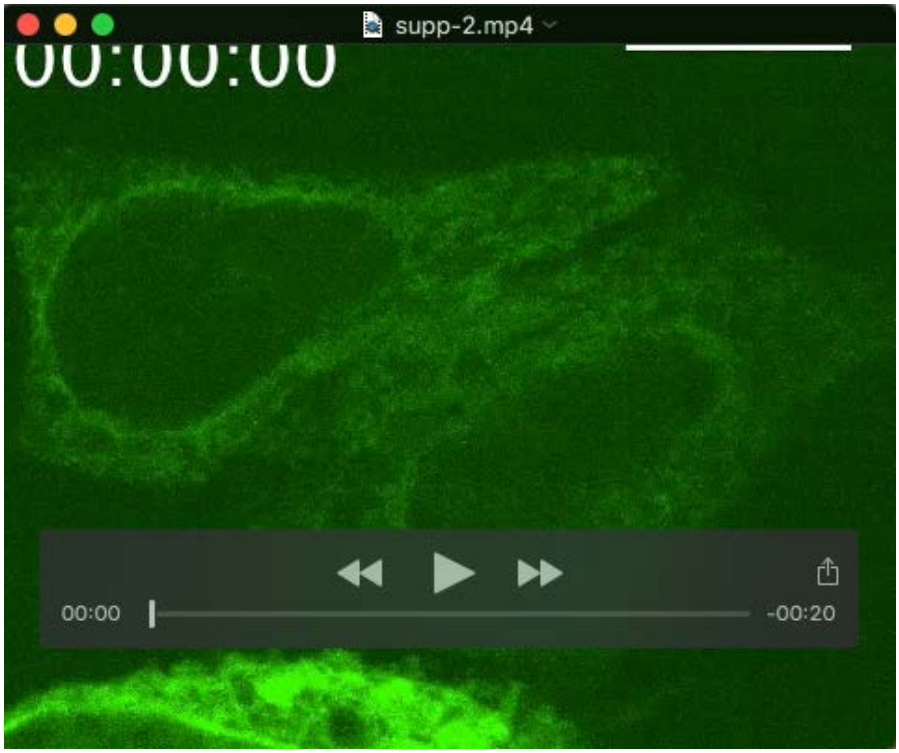

Movie 1. A time-lapse video of the RUSH assay for EGFR-GFP in HeLa cells after biotin treatment. Representative frames are shown in Figure S8B.